

# SIRT1 Regulates the Neurogenic Potential of Neural Precursors in the Adult Subventricular Zone and Hippocampus

Sumiti Saharan, Dhanisha J. **Jhaveri**, and Perry F. Bartlett\*

The Queensland Brain Institute, The University of Queensland, Brisbane, Queensland, Australia

Within the two neurogenic niches of the adult mammalian brain, i.e., the subventricular zone lining the lateral ventricle and the subgranular zone of the hippocampus, there exist distinct populations of proliferating neural precursor cells that differentiate to generate new neurons. Numerous studies have suggested that epigenetic regulation by histone-modifying proteins is important in guiding precursor differentiation during development; however, the role of these proteins in regulating neural precursor activity in the adult neurogenic niches remains poorly understood. Here we examine the role of an NAD<sup>+</sup>-dependent histone deacetylase, SIRT1, in modulating the neurogenic potential of neural precursors in the neurogenic niches of the adult mouse brain. We show that SIRT1 is expressed by proliferating adult subventricular zone and hippocampal neural precursors, although its transcript and protein levels are dramatically reduced during neural precursor differentiation. Utilizing a lentiviral-mediated delivery strategy, we demonstrate that abrogation of SIRT1 signaling by RNAi does not affect neural precursor numbers or their proliferation. However, SIRT1 knock down results in a significant increase in neuronal production in both the subventricular zone and the hippocampus. In contrast, enhancing SIRT1 signaling either through lentiviral-mediated SIRT1 overexpression or through use of the SIRT1 chemical activator Resveratrol prevents adult neural precursors from differentiating into neurons. Importantly, knock down of SIRT1 in hippocampal precursors in vivo, either through RNAi or through genetic ablation, promotes their neurogenic potential. These findings highlight SIRT1 signaling as a negative regulator of neuronal differentiation of adult subventricular zone and hippocampal neural precursors. © 2013 Wiley Periodicals, Inc.

**Key words:** Sirt1; neural precursor cells; adult neurogenesis; epigenetic; neuronal differentiation

Adult neurogenesis is a multistage process regulated by a delicate balance between undifferentiated proliferative neural precursor cells and differentiated neuronal progeny. There are two evolutionarily conserved neurogenic niches in the adult mammalian brain, the subventricular zone (SVZ) that lines the lateral wall of the lateral

ventricle and the subgranular zone (SGZ) that lies within the dentate gyrus of the hippocampus. Numerous regulatory transcription factors involved in stem cell self-renewal and fate regulation have been identified for both of these neurogenic niches (Ballas and Mandel, 2005; Agathocleous et al., 2009; Briscoe, 2009; Wexler et al., 2009). The progression of a neural stem cell to its differentiated progeny requires the silencing of self-renewal genes and the concurrent transcriptional activation of cell-type specific genes. In recent years, the importance of epigenetic mechanisms in orchestrating precise changes in gene expression profile has also become apparent. Epigenetic modifications such as histone acetylation and deacetylation provide a crucial intrinsic mechanism by which the differentiation of stem cells can be regulated (Hsieh and Gage, 2004; Wen et al., 2009; Hirabayashi and Gotoh, 2010; Hsieh and Eisch, 2010), with recent work revealing histone deacetylases (HDACs) to be important for lineage specification in neural stem cells both during development and in the adult brain (Hsieh et al., 2004; Balasubramanian et al., 2006; Lyssiotis et al., 2007; Siebzehnrbubl et al., 2007; Kohyama et al., 2008; Schneider et al., 2008; Yu et al., 2009; Juliandi et al., 2010).

One such HDAC that has been shown to interact with a large number of transcription factors and signaling pathways involved in adult neurogenesis is SIRT1, a class III NAD-dependent histone and protein deacetylase that characteristically inhibits activity of its downstream targets through transcriptional repression (Haigis and Guarente, 2006). During development, SIRT1 is robustly expressed throughout the central nervous sys-

Contract grant sponsor: National Health and Medical Research Council of Australia; Program Contract grant number: 569575; Contract grant sponsor: Estate of Dr. Clem Jones AO

\*Correspondence to: Perry F. Bartlett, Queensland Brain Institute, The University of Queensland, Brisbane, Queensland 4072, Australia. E-mail: p.bartlett@uq.edu.au

Received 23 August 2012; Revised 7 December 2012; Accepted 10 December 2012

Published online 00 Month 2013 in Wiley Online Library (wileyonlinelibrary.com). DOI: 10.1002/jnr.23199

tem, suggesting a role for this sirtuin protein in neuronal development (Sakamoto et al., 2004). In line with this, Prozorovski and colleagues (2008) showed that SIRT1 influences cell fate decisions in embryonic neural precursor cells. Recently, SIRT1 has been shown to regulate pluripotency and differentiation genes in human embryonic stem cells (Calvanese et al., 2010). It has also been found to be important in maintaining an undifferentiated/self-renewing state in mouse embryonic stem cells in vitro (Han et al., 2008). However, despite these lines of evidence for a role of SIRT1 signaling in modulating differentiation of various embryonic pluripotent cell types, its role in adult neurogenesis has not yet been investigated. The present study analyzes the effects of SIRT1 knock down and overexpression on adult neural precursor cells in the SVZ and SGZ. Our results reveal that abrogation of SIRT1 signaling in proliferating neural precursors enhances neuronal differentiation, whereas enhancing SIRT1 activity prevents adult neural precursor cells from generating new neurons. These findings highlight a novel role for SIRT1 signaling in regulating the neurogenic potential of adult precursors in both the SVZ and the SGZ.

## MATERIALS AND METHODS

### Animals

Adult (6–8 weeks of age, except where specifically stated otherwise) male C57Bl/6 mice were used for this study. The animals were housed in filter-top cages with unlimited access to food and water, in a temperature- and humidity-controlled room, and maintained on a 12-hr light/12-hr dark cycle. The *Sirt1*<sup>CO/CO</sup> floxed mouse strain, in which the catalytic domain exon 4 of the *Sirt1* gene is flanked with the loxP sequence, was generated by Li and colleagues (2007) and obtained from The Jackson Laboratory. Mice homozygous for the targeted alleles were maintained on a mixed 129X1/SvJ; C57Bl/6 genetic background. These mice are viable and fertile and express normal levels of Sirt1 protein (Li et al., 2007). To convert the *Sirt1* conditional CO allele into the *Sirt1* knockout KO allele, *Sirt1*<sup>CO/CO</sup> mice were crossed with nestin-Cre transgenic mice (kindly provided by Prof. Linda Richards, Queensland Brain Institute, The University of Queensland), in which the nestin promoter drives Cre expression (Tronche et al., 1999). Animals were treated in accordance with the Australian Code of Practice for the Care and Use of Animals for Scientific Purposes. Ethics approval for all experiments was obtained from the University of Queensland Animal Ethics Committee (QBI/224/10/NHMRC).

### Genotyping

A PCR-based genotyping method was used to identify the *Sirt1* conditional targeted allele (CO) with the following primers (Jackson Laboratory): Sirt1CO: forward 5'-GGT TGA CTT AGG TCT TGT CTG and reverse 5'-CGT CCC TTG TAA TGT TTC CC. The expected band sizes in base pairs (bp) were mutant (CO/CO) = 750 bp, heterozygote (CO/+) = 750 bp and 550 bp, wild-type (+/+) = 550 bp. To genotype for *Sirt1* knockout (post Cre excision), we used

the following primers (Jackson Laboratory): Sirt1KO: forward 5'-AGG CGG ATT TCT GAG TTC GA and reverse 5'-CGT CCC TTG TAA TGT TTC CC. Expected band sizes were null (KO/KO) = 450 bp, wild-type (+/+) = 900 bp. The presence or absence of the nestin-Cre transgene was determined with the following primers (Jennemann et al., 2005): nestin: forward 5'-CCG CTT CCG CTG GGT CAC TGT and reverse 5'-GAC CGG CAA ACG GAC AGA AGC A. A 380-bp band indicated the presence of Cre.

### Primary Neurosphere Cultures

Adult male mice were killed by cervical dislocation; their brains were immediately removed, and the hippocampus or SVZ was dissected in HEPES-buffered minimum essential medium (HEM) consisting of minimum essential medium (Invitrogen, Carlsbad, CA) supplemented with 16 mM HEPES (Sigma-Aldrich, St. Louis, MO) and 100 U/ml penicillin/streptomycin (Invitrogen). SVZ tissue was mechanically chopped using a scalpel blade and then enzymatically digested with 0.1% trypsin-EDTA (Invitrogen) for 7 min at 37°C, followed by a wash with 0.014% w/v trypsin inhibitor (type I-S from soybean; Sigma-Aldrich) dissolved in HEM. The tissue was then centrifuged at 100 rcf for 7 min, after which the pellet was resuspended in 1 ml neurosphere growth medium. Hippocampal tissue was also chopped finely using a scalpel blade and then digested with 1 ml papain (Worthington Biochemical, Lakewood, NJ) for 20 min at 37°C with intermediate agitation provided by gently pipetting four or five times every 6 min. The tissue was then centrifuged at 100 rcf for 7 min, after which the pellet was resuspended in 1 ml Hank's balanced salt solution (HBSS; Sigma-Aldrich). Next, the tissue was centrifuged at 100 rcf for 7 min and resuspended in 1 ml neurosphere growth medium. Both SVZ and hippocampal tissue were then mechanically triturated before being filtered through a 40- $\mu$ m cell sieve (Falcon, BD Biosciences, San Jose, CA). The neurosphere growth medium consisted of mouse NeuroCult NSC Basal Medium plus mouse NeuroCult NSC Proliferation Supplements (Stem Cell Technologies, Vancouver, British Columbia, Canada) containing 2% bovine serum albumin (Invitrogen) and 2  $\mu$ g/ml heparin (Sigma-Aldrich). Epidermal growth factor (EGF; 20 ng/ml purified mouse receptor grade; BD Biosciences), bovine fibroblast growth factor (FGF-2; 10 ng/ml recombinant; Roche, Indianapolis, IN), and 10 U/ml penicillin-G/10 mg/ml streptomycin (Invitrogen) were also included. The cells were plated at a density of approximately one hippocampus or SVZ per 96-well plate (Falcon, BD Biosciences) with 200  $\mu$ l neurosphere medium per well. Primary hippocampal cells and SVZ cells were incubated for 14 and 7 days, respectively, at 37°C in humidified 5% CO<sub>2</sub> to permit neurosphere formation. At the end of this period, the number of neurospheres was counted, and the results were calculated as neurospheres per brain or per total number of cells.

Resveratrol (3,4,5-trihydroxy-trans-stilbene; Sigma-Aldrich) was used as a potential activator of Sirt1. Resveratrol was dissolved in dimethylsulfoxide (DMSO; Sigma) to form a 10 mM stock solution, which was protected from light at all times. For in vitro Resveratrol treatment of SVZ and/or hip-

popocampal neural precursors, the stock solution was dissolved in complete neurosphere growth medium at the time of plating, resulting in the final desired concentration of the drug and a DMSO concentration of 0.2%. For control medium, DMSO was added to complete medium at a final concentration of 0.2%.

### Differentiation of Neurospheres

To provide an adherent surface on which the neurospheres could differentiate, 18-mm round glass coverslips were sterilized and precoated with 15  $\mu$ g/ml poly-L-ornithine (Sigma) and laminin (natural mouse; Invitrogen). Cultured neurospheres (7 days for SVZ neurospheres and 14 days for hippocampal neurospheres) were collected and resuspended in differentiation medium, free from growth factors, which consisted of mouse NeuroCult NSC Basal Medium plus mouse NeuroCult NSC Proliferation Supplements and 10 U/ml penicillin-G/10 mg/ml streptomycin. Induction of neural differentiation was initiated by plating the neurospheres on precoated coverslips in 24-well plates. The neurospheres were then allowed to differentiate for 5–6 days at 37°C in a humidified 5% CO<sub>2</sub> incubator.

### Immunocytochemistry

To assess differentiation potential, the differentiated neurospheres were immersion fixed in 4% paraformaldehyde (PFA) in 0.1 M phosphate-buffered saline (PBS) for 20 min at room temperature. After three rinses in 0.1 M PBS, they were placed in blocking solution, comprising 0.1 M PBS containing 0.1% Triton X-100 (0.1% PTX) and 2% normal goat serum, for 1 hr and then were incubated at 4°C overnight with the neuronal marker  $\beta$ III-tubulin (1:2,000; Promega, Madison, WI) diluted in 0.1% PTX. The neurospheres were then rinsed with 0.1% PTX and incubated for 2 hr at room temperature with Alexa Fluor-conjugated secondary antibodies diluted in 0.1% PTX (1:2,000; Molecular Probes, Eugene, OR). The coverslips were then rinsed with 0.1% PTX, counterstained with the nuclear marker 4,6-diamidino-2-phenylindole (DAPI; 1:1,000), and mounted on glass slides using fluoromount (Dako Cytomation, Carpinteria, CA), before being viewed on a Zeiss Axio-Imager microscope. Images were captured using a digital camera linked to a computer running Zeiss Axiovision software. For quantification, similarly sized neurospheres were used, and the percentage of neurospheres expressing a given marker was estimated. At least 50 neurospheres were counted for each condition.

### Lentiviral Constructs

Single-hairloop RNAs (shRNAs) designed specifically for *Sirt1* were ordered as single-stranded oligonucleotides (Geneworks, Hindmarsh, South Australia, Australia) and annealed in a buffer containing 100 mM Tris HCl (pH 7.5), 1 M NaCl, and 10 mM EDTA. The *Sirt1*shRNA sequence used for our experiments has previously been shown to knock down SIRT1 effectively (Cohen et al., 2004). A random sequence generated by scrambling the nucleotides in the *Sirt1*-specific shRNA sequence, without homology to any known mRNA, was used as a control. shRNAs were then inserted

into the transfer plasmid hCMV.GFP.U6.WPRE (kindly provided by Dr. Nigel McMillan, Diamantina Institute, The University of Queensland), under the U6 promoter. The corresponding oligonucleotides used for generating the *Sirt1* shRNA were *Sirt1*shRNA: forward 5'-TGA AGT TGA CCT CCT CAT TGT TTC AAG AGA ACA ATG AGG AGG TCA ACT TCT TTT TTC and reverse 5'-TCG AGA AAA AAG AAG TTG ACC TCC TCA TTG TTC TCC TGA AAC AAT GAG GAG GTC AAC TTC A, ScramshRNA: forward 5'-TGC GAT TAC GCT TTC GAA TCT TTC AAG AGA AGA TTC GAA AGC GTA ATC GCT TTT TTC and reverse 5'-TCG AGA AAA AAG CGA TTA CGC TTT CGA ATC TTC TCT TGA AAG ATT CGA AAG CGT AAT CGC A.

For SIRT1 overexpression, we made use of the lentiviral transfer plasmid flap-Ub promoter-IRES-GFP-WRE (Dr. Nigel McMillan), containing the ubiquitin promoter, with an IRES site and green fluorescent protein (GFP) to be able to overexpress SIRT1 and fluorescently label the infected cells. To generate the SIRT1 overexpression lentiviral transfer vector, *Sirt1* cDNA was excised out of pUSEamp vector (Millipore, Bedford, MA) with an EcoRI restriction digest, blunted at the ends using Klenow fragment, and ligated with BamHI-digested and blunted flap-Ub promoter-IRES-GFP-WPRE vector.

### Lentiviral Production

We have used third-generation lentiviral vectors, which are derived from human immunodeficiency virus (HIV; Dull et al., 1998). These pMDLg/pRRE, pRSV-Rev and pMD2.VSV-G lentiviral packaging plasmids were kindly provided by Dr. Nigel McMillan. Lentiviral stocks were produced by calcium phosphate transfection into HEK 293T cells, as previously described (Follenzi et al., 2002; Tiscornia et al., 2006). Briefly, supernatants were collected, passed through a 0.45- $\mu$ m filter, and then concentrated by ultracentrifugation. Expression titers were estimated on HEK 293T cells by limiting dilution. The concentrated lentivector titer ranged from  $1 \times 10^9$  to  $1 \times 10^{10}$  transducing units (TU)/ml for each vector. All viral stocks used for injections were diluted to  $1 \times 10^9$  TU/ml using PBS.

### Transfection and Western Blot Analysis

Floating neurospheres were collected in a 10-ml Falcon tube and spun down at 700 rpm for 5 min. The medium was aspirated, and the cells were lysed by the addition of 100  $\mu$ l of a detergent-based cell lysis buffer. Differentiated neurospheres were washed once with ice-cold PBS, lysed with 100  $\mu$ l of lysis buffer, and immediately scraped off the wells. Lysates were transferred to 1.5-ml Eppendorf tubes and spun at 13,000 rcf for 10 min at 4°C. The supernatant was collected and the protein content in cell lysates was determined using the BSA Protein Assay Kit (Bio-Rad, Hercules, CA).

For Western blotting, equal protein amounts of cell lysates were subjected to SDS-PAGE and transferred to a polyvinylidene fluoride membrane (Millipore). The membrane was incubated in blocking solution (0.1 M PBS with 0.1% Tween-20 and 5% nonfat milk powder) for 2 hr before being

incubated overnight at 4°C with primary antibodies against SIRT1 (1:5,000; Millipore) and  $\beta$ -actin (1:5,000; Sigma), diluted in blocking buffer. After washing five times for 5 min in PBS containing 0.1% Tween 20, secondary horseradish peroxidase-conjugated donkey anti-rabbit (1:10,000; Santa Cruz Biotechnology, Santa Cruz, CA) or donkey anti-mouse (1:10,000; Santa Cruz Biotechnology) antibody was added, and the membranes were incubated for 1.5 hr at room temperature. After a final 5-min wash, membranes were exposed to enhanced chemiluminescence detection solution (ECL-Plus; Pierce, Rockford, IL) for 5 min to allow the membrane to develop. For quantification, protein levels were normalized to the levels of  $\beta$ -actin.

#### Reverse-Transcription Followed by Quantitative PCR

The expression of mouse transcripts was determined by reverse transcription of total RNA followed by quantitative PCR analysis (qRT-PCR). After a DNase treatment, 2  $\mu$ g total RNA was reverse transcribed (SuperScript First-Strand Synthesis System) according to the manufacturer's protocol. The quantitative real-time reverse transcriptase PCR (qRT-PCR) reactions were performed on the Rotor-gene 6000 real-time PCR detection system (Corbett Lifesciences, Valencia, CA) using the SYBR Green mix (Bio-Rad) with the following primers (supplied by Geneworks): Sirt1: forward 5'-GCA GAT TAG TAA GCG GCT TGA G and reverse 5'-GGG CCT CTC CGT ATC ATC TT,  $\beta$ -actin: forward 5'-CAC ACT GTG CCC ATC TAC GA and reverse 5'-GTG GTG GTG AAG CTG TAG CC.

PCR runs were performed using the following thermal cycling conditions: 3 min at 95°C followed by 40 cycles of 1 sec at 95°C for denaturation, 15 sec at 60°C for primer annealing, and 5 sec at 72°C for elongation. A melt curve from 70°C to 99°C (0.5°C/sec) was performed to analyze the specificity of the primers and the quality of the product. Sample reactions were run in triplicate. For each set of triplicates, the mean value for each gene transcript was determined, and the obtained values were normalized against the housekeeping gene  $\beta$ -actin to calculate the fold changes (treatment vs. untreated control) in relative gene expression. A PCR control on RNA that had not been reverse transcribed was included at all times to make sure that no genomic DNA had been amplified.

#### Lentiviral Infection

For in vitro infection of neural precursor cells, primary dissociated cells were obtained as previously described and then plated in 24-well plates at a density of  $2 \times 10^4$  cells/ml/well. The plates were kept in a humidified 5% CO<sub>2</sub>/37°C tissue culture incubator. At 6 hr postplating, 2  $\mu$ l of the respective lentiviral stocks was added directly to each well (approximately  $2 \times 10^6$  TU/well), after which the plates were returned to the incubator. Infection efficiencies of at least 90% were obtained as assessed by the number of GFP-positive neurospheres formed.

To study the influence of knock down of SIRT1 signaling on adult hippocampal progenitors in vivo, 10-week-old male C57BL/6 mice were anesthetized with a mixture of ke-

tamine (100 mg/kg; Apex Laboratories, Farmingdale, NY) and the muscle relaxant xylazine (5 mg/kg; Bayer). Mice were fixed in a stereotaxic apparatus (David Kopf Instruments, Tujunga, CA) using ear and nose bars, and a small midline incision was made to expose the skull. A 20- $\mu$ l glass capillary was filled with lentiviral stock, attached to a manual picoliter injector and set to the following coordinates relative to Bregma (in mm): anterior-posterior -2, mediolateral +1.5, dorsoventral -2. The skull was drilled at these coordinates to expose the brain, and the capillary was very slowly (over 3-5 min) inserted into the brain to the required depth. At a flow rate of approximately 0.1  $\mu$ l/min, 0.5-1  $\mu$ l viral suspension was injected into the brain. After the injection was finished, the capillary was left in place for up to 5 min. The capillary was then slowly retracted, and the skull hole was filled with bone wax, after which the skin was glued with tissue glue and the mouse was placed on a heating pad to recover and then returned to the home cage. The mice were perfused with ice-cold 4% paraformaldehyde (PFA) 2 weeks postsurgery.

#### BrdU Pulse Chase Assay

To analyze the neurogenic potential of neural precursors in vivo, we performed a 5-bromo-2'-deoxyuridine (BrdU) pulse chase assay. Mice were given intraperitoneal pulses of 100 mg/kg BrdU every 12 hr for 2 days and then sacrificed 1 week after the last BrdU pulse. The number of BrdU-expressing cells provided an index of proliferation, and the percentage of BrdU-expressing cells that colabeled for neuronal markers gave a measure of the neurogenic potential of the dividing cells. Alternatively, to look at the survival of dividing cells, the mice were given intraperitoneal injections of 100 mg/kg BrdU every 12 hr for 3 days and were sacrificed 2 weeks after the last BrdU dose. The number of BrdU-expressing cells present after 2 weeks provided an estimate of the survival rate of dividing cells.

#### Immunohistochemical Analysis

Adult animals were transcardially perfused with chilled 0.1 M PBS followed by 4% PFA. The brains were removed and postfixed overnight in 4% PFA, followed by washes in PBS. The brain tissue was cryoprotected by incubation in 30% w/v sucrose in 0.1 M PBS overnight, after which 40- $\mu$ m sections were cut using a freezing microtome. Every fourth slice was used for immunohistochemical analysis. The sections were permeabilized by washing three times with PBS containing 0.3% Triton X (0.3% PTX), blocked in 0.3% PTX containing 3% normal goat serum for 1 hr, then labeled with the following primary antibodies: mouse anti-SIRT1 (1:500; Chemicon, Temecula, CA), rabbit anti-SIRT1 (1:1,000; Millipore), the immature neuronal marker rabbit antidoublecortin (DCX; 1:500; Sapphire Bioscience, Waterloo, New South Wales, Australia), the astroglial marker rabbit antigliab fibrillar acidic protein (GFAP; 1:500; Dako Cytomation), and the proliferative marker rabbit anti-Ki67 (1:500; Novacastra, Buffalo Grove, IL). BrdU immunohistochemistry was performed essentially as described previously (Kulkarni et al., 2002). In brief, this involved DNA denaturation and acid hy-

drololysis followed by overnight incubation with mouse anti-BrdU antibody (1:500; Roche). After incubation with the respective primary antibodies, the sections were washed three times using 0.1% PTX and incubated for 2 hr at room temperature with Alexa Fluor-conjugated secondary antibodies (1:2,000; Molecular Probes) and DAPI (1:1,000). The sections were mounted using Fluoromount (Dako Cytomation) and viewed on a Zeiss Axio-Imager microscope. Optical sectioning was achieved using ApoTome and images were captured using a digital camera linked to a computer running Zeiss Axiovision software. For quantification, the number of cells expressing a given marker along the SGZ of the dentate gyrus was counted.

**Statistical Analysis**

All results are presented as mean ± SEM. Group comparisons were made with the Student's *t*-test, and *P* < 0.05 was considered significant. In addition, for comparisons among three or more groups, a one-way ANOVA was performed to test for significance. In some cases, such as the Resveratrol dose-response study, Dunnett's posttest analysis was performed to compare all groups with the control. In experiments in which there were two variables, such as assessing the effect of Resveratrol treatment on neuron distribution, a two-way ANOVA with Bonferroni's post hoc analysis was used to determine the groups that were statistically significant. All data were analyzed in the Prism statistical package.

**RESULTS**

**SIRT1 Is Expressed in the Adult Neurogenic Niches**

To determine whether SIRT1 is expressed in the neurogenic niches of the adult mouse brain, we stained coronal sections containing the SVZ and hippocampus with a SIRT1-specific antibody. Strong SIRT1 expression was observed in the SVZ, along the lateral wall of the lateral ventricle (Fig. 1A). In the adult hippocampus, SIRT1 was expressed throughout the dentate gyrus, including the SGZ (Fig. 1B, inset). To determine whether SIRT1 was expressed in the dividing cells within this region, we colabeled SIRT1-positive cells with the proliferation marker Ki67. All Ki67-expressing cells examined in the SVZ ( $95.75 \pm 3.57$  cells/section; *n* = 3 sections per brain, three brains; Fig. 1C) and SGZ ( $8.74 \pm 1.93$  cells/section; *n* = 8 sections per brain, three brains; Fig. 1D) expressed SIRT1. To confirm that SIRT1 was indeed expressed by neural precursors, the expression of SIRT1 was also examined in isolated neural precursors derived from both the SVZ and the hippocampus. Neural precursors, when cultured in vitro in the presence of mitogens, give rise to neurospheres (Reynolds and Weiss, 1992). High levels of SIRT1 expression were observed in the majority of cells within proliferative neurospheres derived from both the SVZ and the hippocampus (Fig. 1E). In contrast, low SIRT1 immunoreactivity was observed in differentiated neurospheres (Fig. 1E), suggesting that SIRT1 levels may decrease during differentiation. To investigate this

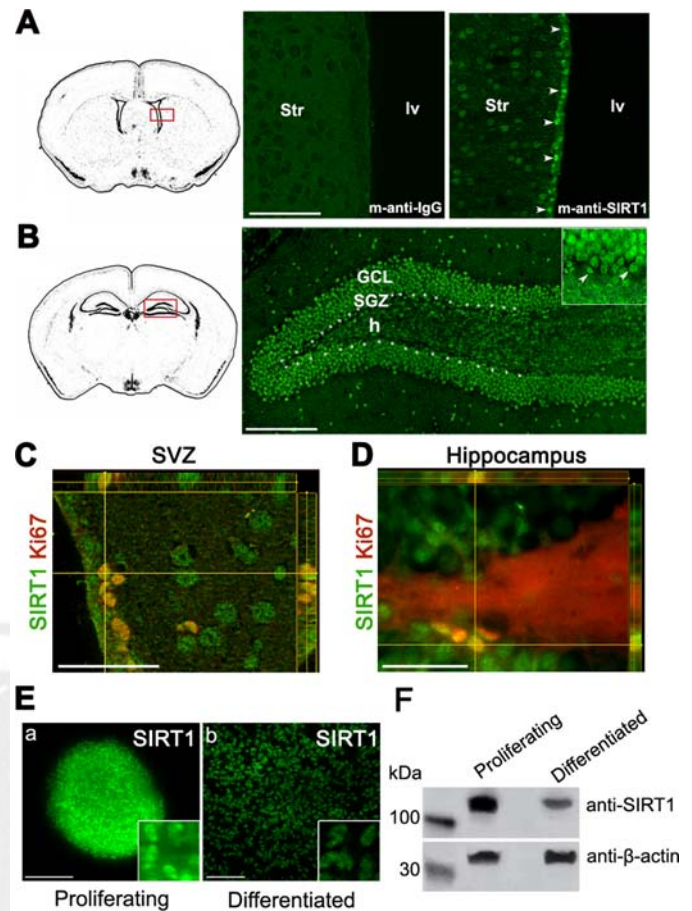


Fig. 1. SIRT1 is expressed by proliferating precursors in the adult neurogenic niches. Adult mouse coronal brain sections stained with anti-SIRT1 antibody (green). Schematics of coronal sections through the mouse brain illustrating the imaged area for the SVZ (A) and hippocampus (B). A: SIRT1-expressing cells were found all along the lateral wall of the SVZ (arrowheads). Control antibody (anti-IgG) did not label any cells in the SVZ. B: In the hippocampus, SIRT1 staining was seen throughout the dentate gyrus, including the SGZ (inset; white arrowheads). Proliferating cells labeled with Ki67 in the SVZ (C) and SGZ (D) express SIRT1 (green). E: SIRT1 expression (green) in proliferating (a) and differentiated (b) SVZ neurospheres. F: Western blot analysis of the protein extracts from proliferating and differentiated neurospheres using anti-SIRT1 and anti-β-actin antibodies. SIRT1 protein was downregulated during differentiation. GCL, granule cell layer; lv, lateral ventricle; SGZ, subgranular zone; Str, striatum; SVZ, subventricular zone; h, hilus. Scale bars = 100 μm in A,B; 40 μm in C,D.

F1

COLOR

AQ1

further, we quantified the protein as well as the mRNA transcript levels of *Sirt1* in adult SVZ neurospheres in the proliferative vs. the differentiative phases. A significant 73.65% reduction in SIRT1 protein was observed in differentiated neurospheres compared with proliferating neurospheres (Fig. 1F). To determine whether this reduction in the levels of SIRT1 protein was due to a decrease in transcription of *Sirt1*, we measured *Sirt1* mRNA levels using quantitative reverse transcriptase

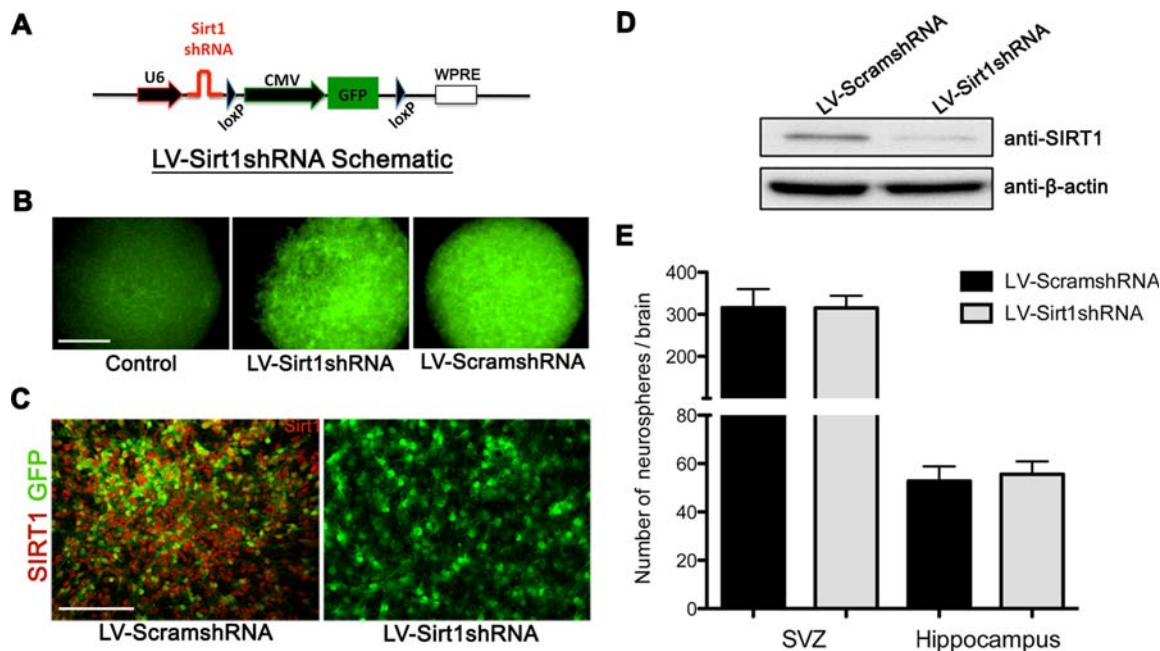


Fig. 2. Lentivirus-mediated knock down of SIRT1 does not affect precursor proliferation. Recombinant lentiviral particles were generated, SIRT1 shRNA (or scrambled shRNA) being expressed under the U6 promoter and the reporter gene GFP driven under the CMV promoter as shown in a schematic (A). B: Seven days after lentiviral infection of primary neural precursor cells, robust GFP expression was seen in neurospheres. C: Differentiated neurospheres immunostained for lentivirus-infected cells (GFP, green) and SIRT1 (red). SIRT1 immu-

noactivity was absent in LV-Sirt1shRNA-expressing neurospheres. D: Western blot analysis of primary neurospheres infected with LV-ScramshRNA and/or LV-Sirt1shRNA showed effective knock down of SIRT1 with SIRT1-specific shRNA.  $\beta$ -Actin served as a loading control. E: Expression of LV-ScramshRNA or LV-Sirt1shRNA in SVZ and hippocampal neural precursors had no effect on neurosphere numbers. Data are represented as mean  $\pm$  SEM of three experiments.  $P > 0.05$ . LV, lentiviral particles. Scale bars = 25  $\mu$ m.

PCR (qRT-PCR) and found a 10.09-  $\pm$  0.78-fold decrease in *Sirt1* mRNA levels in differentiated neurospheres compared with proliferating neurospheres (Student's *t*-test,  $P < 0.001$ ).

### SIRT1 Knock Down Does Not Affect SVZ and Hippocampal Neural Precursor Numbers or Their Proliferation but Enhances Their Neuronal Differentiation

To address the role of SIRT1 in regulating neural precursors, we designed a third-generation lentiviral vector expressing a reporter gene, GFP and SIRT1-specific shRNA (LV-Sirt1shRNA; Fig. 2A). A lentiviral vector expressing a scrambled shRNA sequence (LV-ScramshRNA) was also generated to serve as a control to eliminate nonspecific effects of shRNA production within infected cells. The lentiviral backbone vector (LV-GFP) served as an additional experimental control. The infection efficacy of the resulting lentiviral particles was found to be at least 90% as assessed by the number of SVZ-derived GFP-expressing neurospheres (Fig. 2B). When SVZ neurospheres infected with LV-Sirt1shRNA neurospheres were stained for SIRT1, very little, if any, SIRT1 expression was observed (Fig. 2C). Lentiviral-mediated knock down of SIRT1 was also confirmed by Western blot analysis of protein extracts from

Sirt1shRNA-infected and control ScramshRNA-infected neurospheres. The SIRT1 protein in the neurospheres was effectively reduced by 74.42% (Fig. 2D).

Having established successful knock down of SIRT1 in neural precursors, we investigated its effect on neural precursor numbers by performing the neurosphere assay with SVZ-derived as well as hippocampal-derived precursors. LV-Sirt1shRNA-mediated SIRT1 knock down did not affect the number of neurospheres obtained from either SVZ- or hippocampal-derived neural precursors (Student's *t*-test,  $P > 0.05$ ; Fig. 2E), suggesting that SIRT1 has no regulatory effect on the number of activated neural precursors. Furthermore, Sirt1 knock down did not affect the diameter of the SVZ- or hippocampal-derived neurospheres (data not shown), suggesting that SIRT1 did not affect the proliferative capacity of the precursors.

Next, we addressed whether SIRT1 signaling alters the differentiation potential of neural precursors (Fig 3A). In SVZ-derived differentiated neurospheres infected with LV-Sirt1shRNA, there was a twofold increase in the percentage of  $\beta$ III-tubulin-expressing neurospheres compared with the control LV-GFP- or LV-ScramshRNA-infected neurospheres (one-way ANOVA,  $P < 0.001$ ; Fig. 3B). Upon quantification, a significant increase in the average numbers of neurons per differen-

COLOR

F2

F3

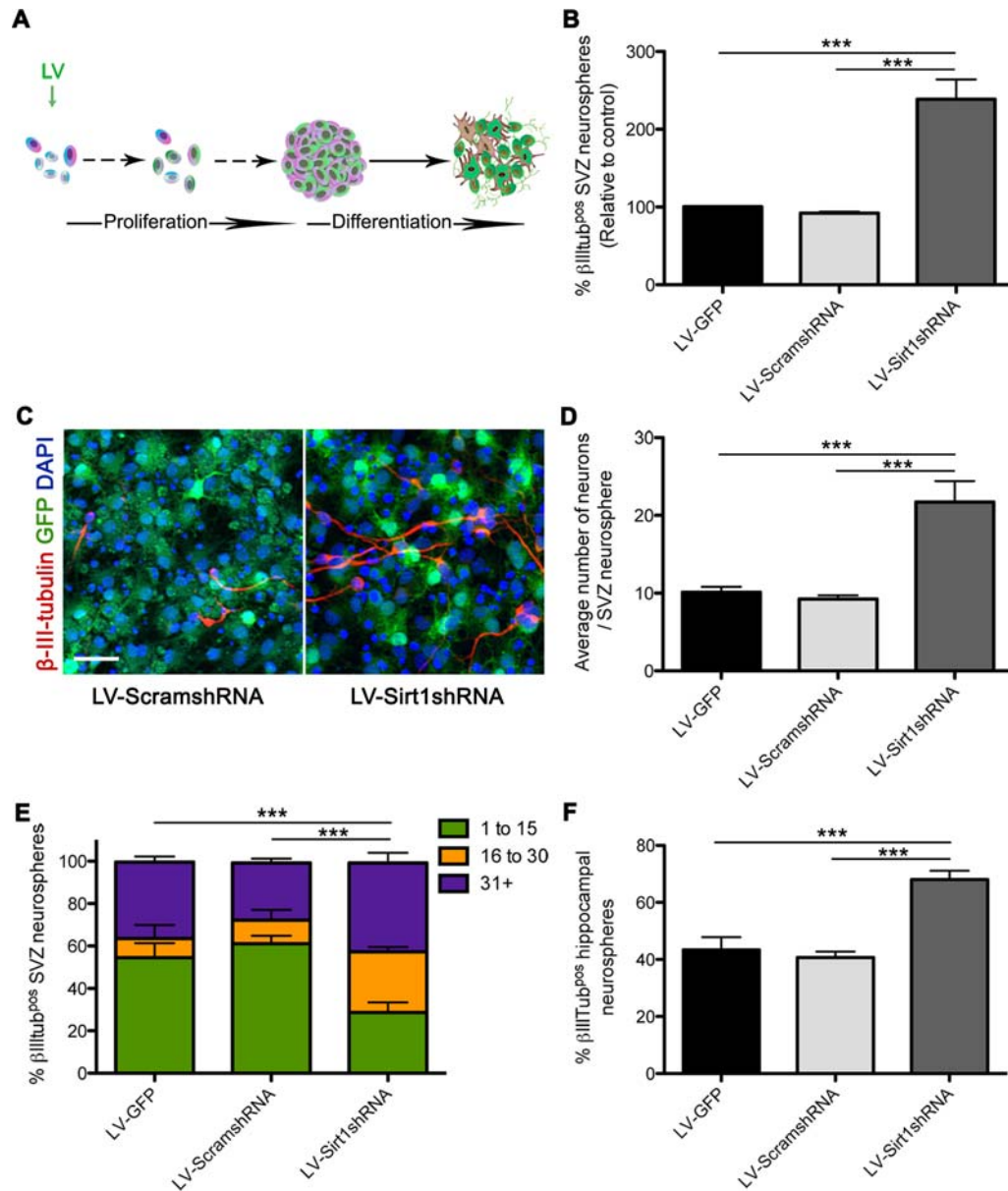


Fig. 3. SIRT1 knock down increases the neurogenic potential of neural precursors. **A:** Diagram showing the experimental strategy. **B:** The proportion of differentiated SVZ neurospheres expressing the neuronal marker  $\beta$ III-tubulin was significantly higher in neurospheres infected with LV-Sirt1shRNA than in LV-GFP- and LV-ScramshRNA-infected control neurospheres. **C:** Representative images showing differentiated SVZ neurospheres expressing LV-ScramshRNA or LV-Sirt1shRNA. Note the increased number of  $\beta$ III-tubulin-expressing neurons in LV-Sirt1shRNA-expressing neuro-

spheres. **D:** The average number of neurons present per neurosphere also increased with SIRT1 knock down. **E:** Distribution profile based on the percentage of neurospheres containing fewer than 15 (green), 16–30 (orange), and more than 30 (purple) neurons. **F:** Percentage of total differentiated hippocampal neurospheres expressing  $\beta$ III-tubulin. LV-Sirt1shRNA-infected hippocampal precursors gave rise to a higher proportion of  $\beta$ III-tubulin-expressing neurospheres. Data are represented as mean  $\pm$  SEM of three experiments. \*\*\* $P < 0.001$ . LV, lentiviral particles. Scale bar = 25  $\mu$ m.

tiated neurosphere was found in LV-Sirt1shRNA-infected neurospheres compared with the controls (one-way ANOVA,  $P < 0.001$ ; Fig. 3C,D). Interestingly, further analysis revealed a shift in distribution based on the number of neurons contained per neurosphere, with 71.4% of LV-Sirt1shRNA neurospheres containing more

than 15 neurons compared with only 45.5% and 38.4% of the LV-GFP and LV-ScramshRNA controls, respectively (two-way ANOVA,  $P < 0.001$ ; Fig. 3E).

To determine whether SIRT1 also regulated the neuronal differentiation of hippocampal-derived neural precursors, we repeated the in vitro SIRT1 knock down

COLOR

study. Similarly to our SVZ findings, SIRT1 knock down in hippocampus-derived precursors also significantly increased the number of differentiated neurospheres containing  $\beta$ III-tubulin-expressing neurons compared with controls (one-way ANOVA,  $P < 0.001$ ; Fig. 3F). However, because a hippocampal neurosphere contains fewer neurons (one or two) than an SVZ-derived neurosphere, we were unable to perform a detailed distribution analysis. Nevertheless, taken together, our data suggest that SIRT1 signaling may be a common mechanism that regulates the neurogenic potential of both SVZ- and hippocampal-derived neural precursors.

### SIRT1 Overexpression Does Not Affect the Activity or Proliferation of SVZ- and Hippocampal-Derived Neural Precursors but Decreases Their Neurogenic Potential

Having demonstrated that SIRT1 knock down enhances neuronal differentiation, we next questioned whether SIRT1 overexpression was sufficient to inhibit neuronal differentiation. To address this, we designed a lentiviral construct overexpressing SIRT1 under the ubiquitin promoter (LV-Sirt1-IRES-GFP). LV-IRES-GFP was used as a control. Overexpression of SIRT1 was confirmed by Western blot analysis of protein extracts from infected SVZ neurospheres and was found to result in a 4.24-fold increase in SIRT1 protein levels (Fig. 4A). We then examined the effect of SIRT1 overexpression on the neurosphere-generating capacity of SVZ and hippocampal neural precursors and found no effect on the number of neurospheres derived from either the SVZ or the hippocampus (Student's  $t$ -test,  $P > 0.05$ ; Fig. 4B), suggesting that overexpression of SIRT1 did not affect neural precursor numbers. Furthermore, SIRT1 overexpression had no effect on neurosphere size (data not shown), affirming that SIRT1 did not affect the proliferative capacity of neural precursors. Next, we examined the effect of increasing SIRT1 levels on the neurogenic potential of precursors. This revealed an approximate 65% reduction in the number of differentiated  $\beta$ III-tubulin-expressing SVZ neurospheres derived from LV-Sirt1-IRES-GFP-infected neural precursors (Student's  $t$ -test,  $P < 0.001$ ; Fig. 4C). Hippocampal neurospheres overexpressing SIRT1 showed a similar 60% reduction in neuronal differentiation compared with controls (Student's  $t$ -test,  $P < 0.01$ ; Fig. 4C). These data suggest that overexpression of SIRT1 in neural precursors is sufficient to block their neuronal differentiation.

### Activation of SIRT1 Signaling Through Resveratrol Decreases the Neuronal Differentiation of Neural Precursors In Vitro

Having demonstrated that overexpression of SIRT1 protein led to inhibition of neuronal differentiation, we next questioned whether enhancing the deacetylase activity of SIRT1 would be sufficient to produce a similar effect. For this we used Resveratrol, a small-molecule activator of SIRT1 that acts by enhancing the

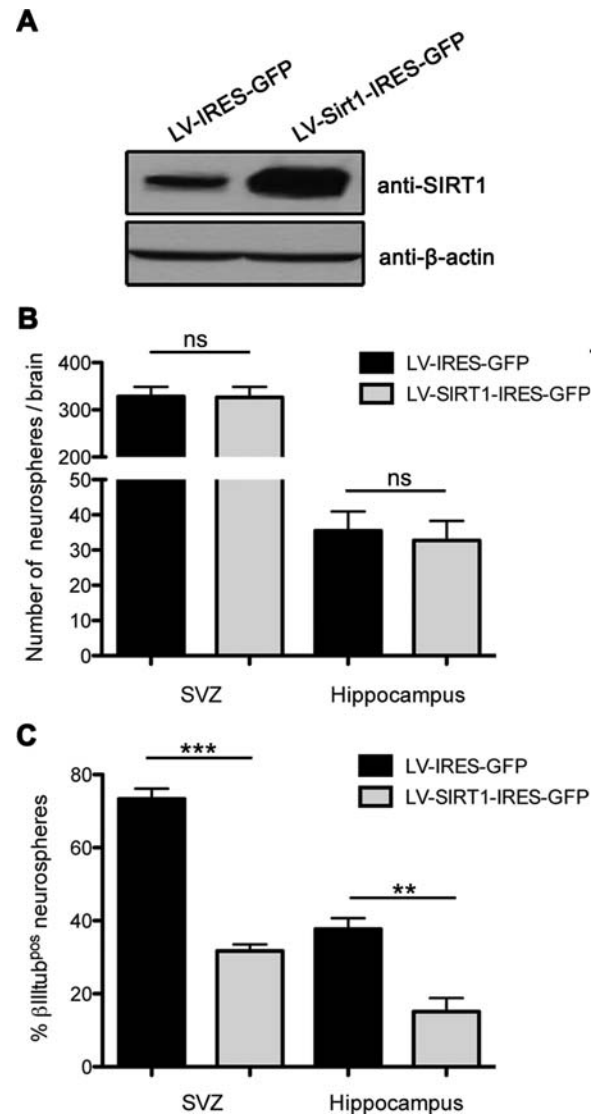


Fig. 4. SIRT1 overexpression inhibits neural precursors from differentiating into neurons. **A:** Western blot analysis showing SIRT1 overexpression in SVZ neurosphere lysate infected with LV-SIRT1-IRES-GFP compared with LV-IRES-GFP-infected neurosphere lysate.  $\beta$ -Actin was the total protein loading control. **B:** Quantification of the number of primary neurospheres obtained from SVZ and hippocampal precursors infected with SIRT1-overexpressing lentiviral particles. SIRT1 overexpression did not affect the number of SVZ or hippocampal neural precursors. **C:** Quantification of the proportion of differentiated SVZ and hippocampal neurospheres expressing the neuronal marker  $\beta$ III-tubulin. Neurospheres overexpressing SIRT1 had significantly reduced neurogenic potential compared with neurospheres expressing the control GFP construct. Data are represented as mean  $\pm$  SEM of three experiments. ns,  $P > 0.05$ , \*\* $P < 0.01$ , \*\*\* $P < 0.001$ .

affinity of SIRT1 for its substrates, increasing its enzymatic activity by up to eightfold (Howitz et al., 2003; Borra et al., 2005). We first evaluated the neurosphere-generating capacity of neural precursors in the presence



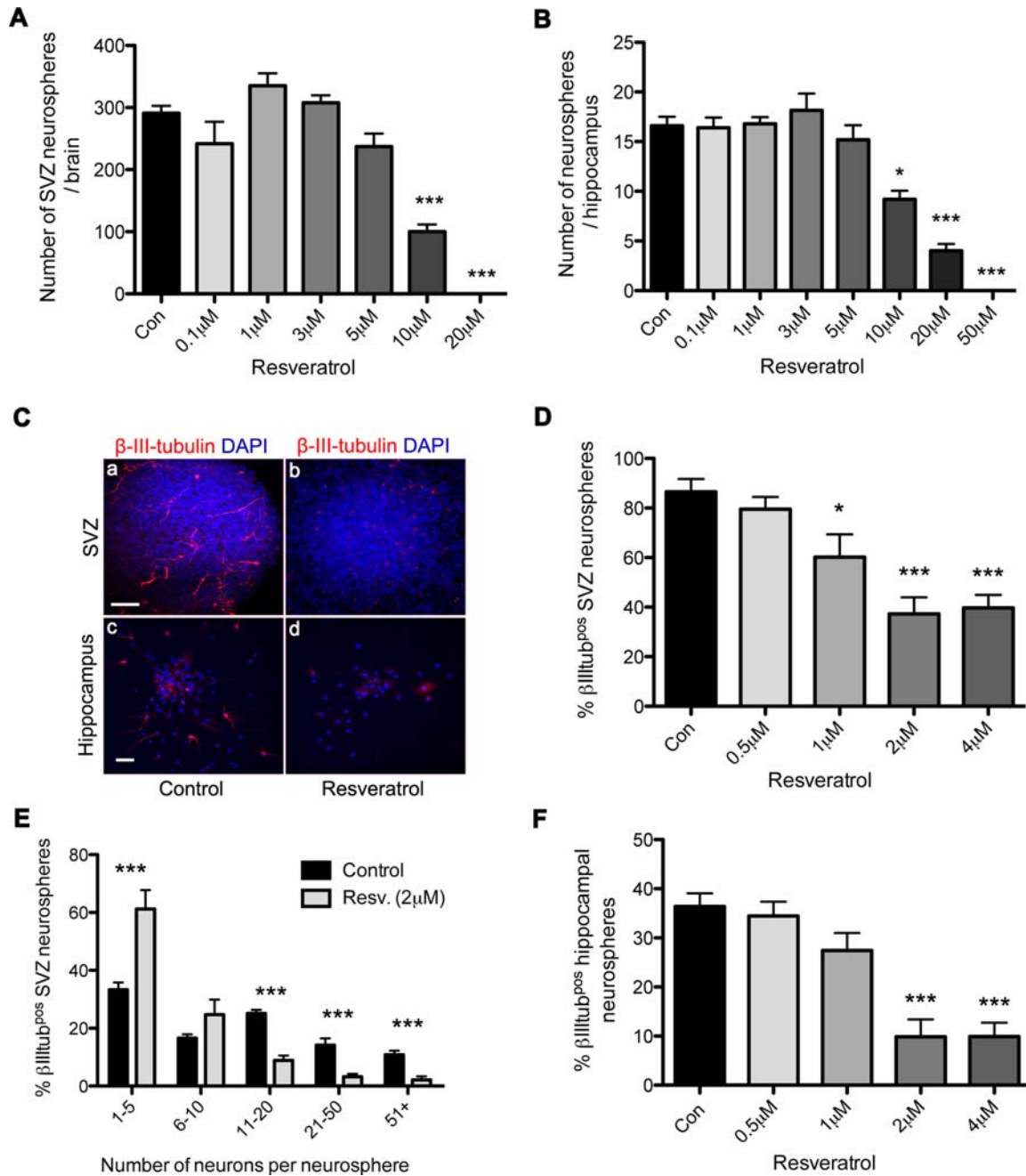


Fig. 5. Resveratrol reduces the number of neurons derived from differentiated adult neurospheres. Effect of Resveratrol on the neurosphere-generating capacity of SVZ (A) and hippocampal (B) precursors. C: Representative images showing differentiated SVZ (a,b) and hippocampal (c,d) neurospheres cultured in the presence of 2  $\mu$ M Resveratrol (a,c) or 0.2% DMSO (b,d). Note the absence of  $\beta$ III-tubulin-expressing neurons (red) in the

Resveratrol-treated neurospheres. D: Proportion of differentiated SVZ neurospheres expressing  $\beta$ III-tubulin. E: Neurosphere distribution based on the number of  $\beta$ III-tubulin-positive neurons per neurosphere. F: Proportion of differentiated hippocampal neurospheres expressing  $\beta$ III-tubulin. Data are represented as mean  $\pm$  SEM of four experiments. \* $P < 0.05$ , \*\*\* $P < 0.001$ . Scale bars = 40  $\mu$ m.

of increasing concentrations of Resveratrol. Resveratrol has previously been shown to mediate Sirt1-dependent functions in vitro at low concentrations of 0.1–5  $\mu$ M (Fremont, 2000; Prozorovski et al., 2008; Pervaiz and

Holme, 2009; Wallenborg et al., 2009). At these concentrations, Resveratrol did not have a significant effect on either SVZ- or hippocampus-derived neurosphere numbers (one-way ANOVA,  $P > 0.05$ ; Fig. 5A,B).

F5

COLOR

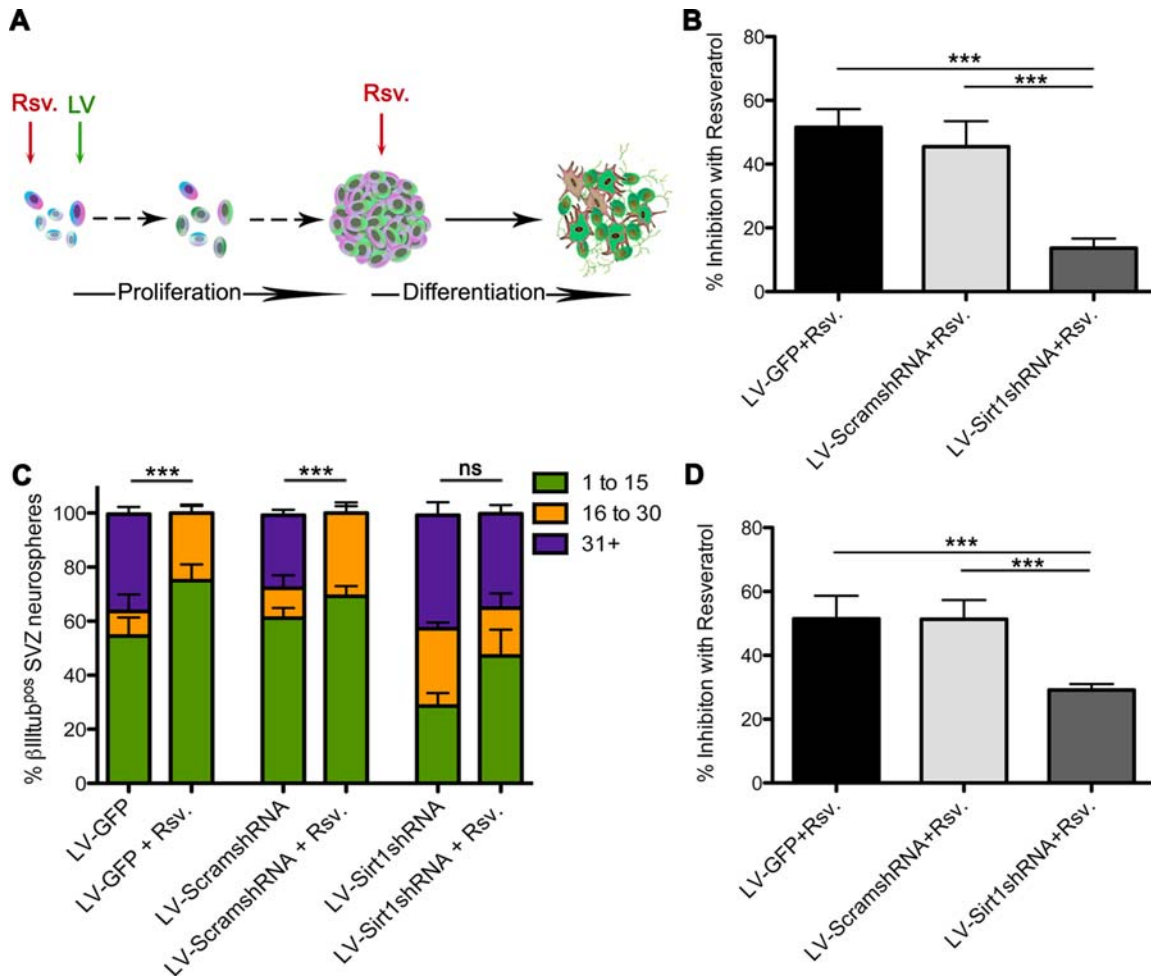


Fig. 6. SIRT1 knock down rescues Resveratrol-mediated neuronal inhibition in vitro. **A:** Schematic diagram showing the experimental strategy. **B:** SIRT1 knock down rescued the inhibition of neuronal differentiation caused by Resveratrol treatment of SVZ-derived precursors. **C:** Neurosphere distribution profiles based on the percentage of SVZ neurospheres containing fewer than 15

(green), 16–30 (orange), and more than 30 (purple) neurons. **D:** SIRT1 knock down in hippocampal neurospheres significantly rescued the Resveratrol-induced reduction in neuronal differentiation. Data are represented as mean  $\pm$  SEM of three experiments. ns,  $P > 0.05$ , \*\*\* $P < 0.001$ . LV, lentiviral particles; Rsv, Resveratrol.

However, at concentrations of 10  $\mu$ M and higher, Resveratrol decreased neurosphere numbers in a concentration-dependent manner (one-way ANOVA,  $P < 0.001$ ; Fig. 5A,B).

Next, we assayed the effect of Resveratrol (0.1–4  $\mu$ M) on neural precursor differentiation. When SVZ-derived neural precursors were cultured and subsequently differentiated in the presence of Resveratrol, a dose-dependent reduction in the percentage of differentiated SVZ neurospheres containing  $\beta$ III-tubulin-expressing neuronal cells was observed (one-way ANOVA,  $P < 0.001$ ; Fig. 5C,D). Furthermore, we observed a significant reduction in the number of  $\beta$ III-tubulin-expressing neurons in neurospheres grown and differentiated in the presence of 2  $\mu$ M Resveratrol, with 92.7% of Resveratrol-treated neurospheres containing fewer than 10 neurons compared with 52.6% of control neurospheres

(two-way ANOVA  $P < 0.001$ ; Fig. 5E). In the case of hippocampal neural precursors, the proportion of differentiated hippocampal neurospheres that produced  $\beta$ III-tubulin-expressing neurons was also markedly decreased in the presence of 2  $\mu$ M and 4  $\mu$ M Resveratrol (one-way ANOVA  $P < 0.001$ ; Fig. 5C,F).

To ascertain whether this Resveratrol-induced inhibition was mediated through a Sirt1-dependent mechanism, we infected Resveratrol-treated neural precursors with LV-GFP, LV-ScramshRNA, or LV-Sirt1shRNA (Fig. 6A). SIRT1 knock down in SVZ-derived neural precursors significantly rescued the inhibitory effects of Resveratrol, producing only a 13% decrease in  $\beta$ III-tubulin-expressing neurospheres compared with an approximate 50% reduction in SVZ-derived precursors infected with control LV-GFP or LV-ScramshRNA (one-way ANOVA,  $P < 0.001$ ; Fig. 6B). In addition,

F6

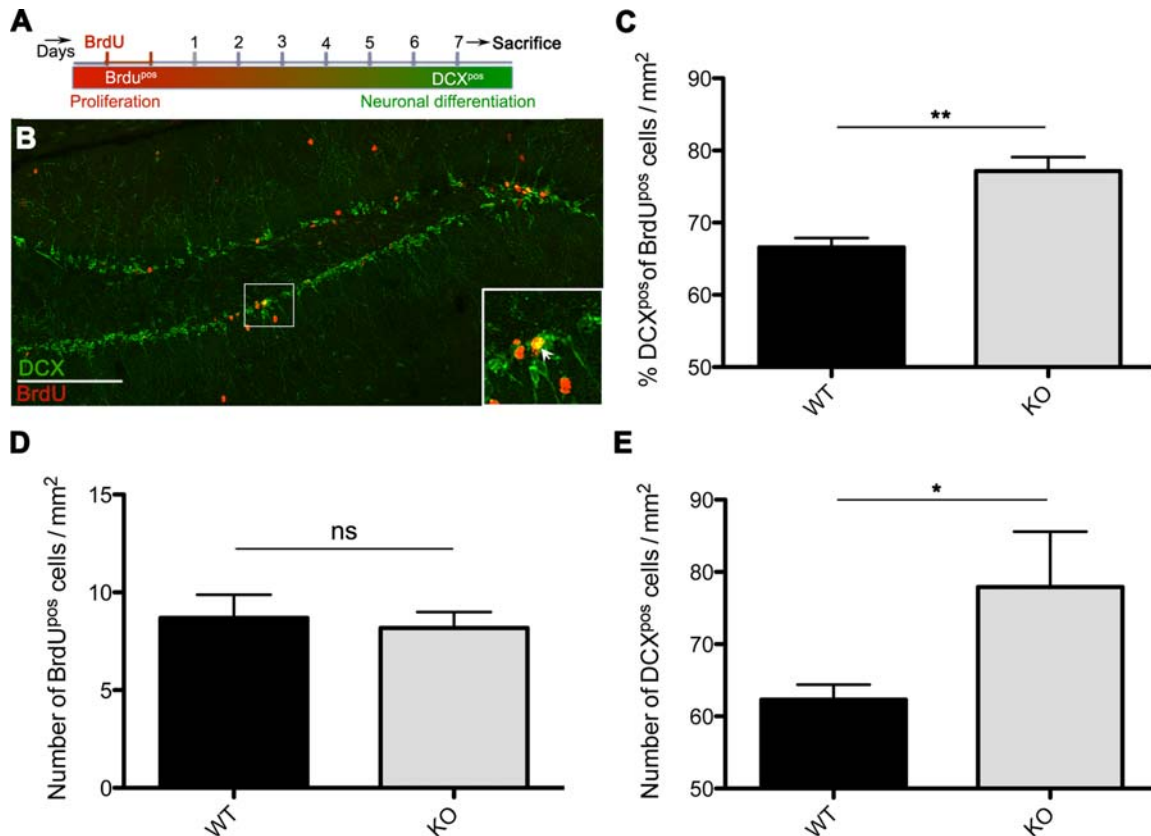


Fig. 7. SIRT1 loss-of-function increases adult neurogenesis in the SGZ. **A:** Representative schematic showing the BrdU injection paradigm; 100 mg/kg BrdU was administered twice per day for 2 days, and the mice were sacrificed after 7 days. The proportion of BrdU-labeled cells that colabeled with DCX was quantified in the SGZ of Sirt1KO and WT animals. **B:** Representative image showing colabeling with DCX (green) and BrdU (red) in the SGZ. **Inset** shows a magnified image of a cell colabeled for BrdU and DCX (arrow). **C:**

The proportion of BrdU-positive cells expressing DCX was significantly increased in Sirt1KO animals. **D:** The average number of BrdU-positive cells per square millimeter of SGZ was not affected by SIRT1 ablation. **E:** A significant increase in the number of DCX-expressing newborn neurons was observed per square millimeter of SGZ in SIRT1 KO compared with WT control. Data are represented as mean  $\pm$  SEM of at least four animals per condition. ns,  $P > 0.05$ , \* $P < 0.05$ , \*\* $P < 0.01$ . Scale bar = 100  $\mu$ m.

COLOR

quantification of the number of neurons produced per neurosphere revealed a dramatic rescue of neuronal numbers by SIRT1 knock down (two-way ANOVA,  $P < 0.001$ ; Fig. 6C). For instance, in LV-GFP- and LV-ScramshRNA-infected neurospheres, Resveratrol treatment resulted in no neurospheres containing more than 30 neurons compared with 36% and 26% of untreated LV-GFP- and LV-ScramshRNA-infected neurospheres, respectively (Fig. 6C). Sirt1shRNA rescued this Resveratrol-induced inhibition of neuronal differentiation, with 32% of Resveratrol-treated LV-Sirt1shRNA-infected neurospheres containing more than 30 neurons (Fig. 6C). Furthermore, we also examined whether SIRT1 knock down was able to rescue the neurogenic potential of Resveratrol-treated hippocampal neurospheres. Indeed, SIRT1 knock down with LV-Sirt1shRNA significantly rescued the Resveratrol-mediated inhibitory effect, relative to Resveratrol-treated control LV-GFP- and LV-ScramshRNA-infected neurospheres (one-way ANOVA,  $P < 0.001$ ; Fig. 6D). Together, these data

suggest that the Resveratrol-induced reduction in neuronal differentiation of SVZ- and hippocampal-derived neural precursors is dependent on SIRT1 signaling.

### Genetic Ablation of SIRT1 Enhances Neurogenesis

So far, we have demonstrated that SIRT1 signaling was both necessary and sufficient to regulate neuronal differentiation of neural precursors in vitro. We next sought to determine whether SIRT1 affected the neurogenic potential of neural precursors in vivo. To this end, we generated mutant mice lacking the SIRT1 catalytic domain in a brain-specific manner by crossing *Sirt1* floxed transgenic mice (Li et al., 2007) with nestin-Cre transgenic mice (Tronche et al., 1999). SIRT1 knockout was confirmed by performing a Western blot analysis with protein lysates of SVZ-derived neurospheres from *Sirt1*<sup>+/+</sup>, *Sirt1*<sup>KO/+</sup>, and *Sirt1*<sup>KO/KO</sup> adult mice (data not shown). As expected, the *Sirt1*<sup>+/+</sup> neurosphere lysate showed a protein band at 110 kDa. *Sirt1*<sup>KO/+</sup> and

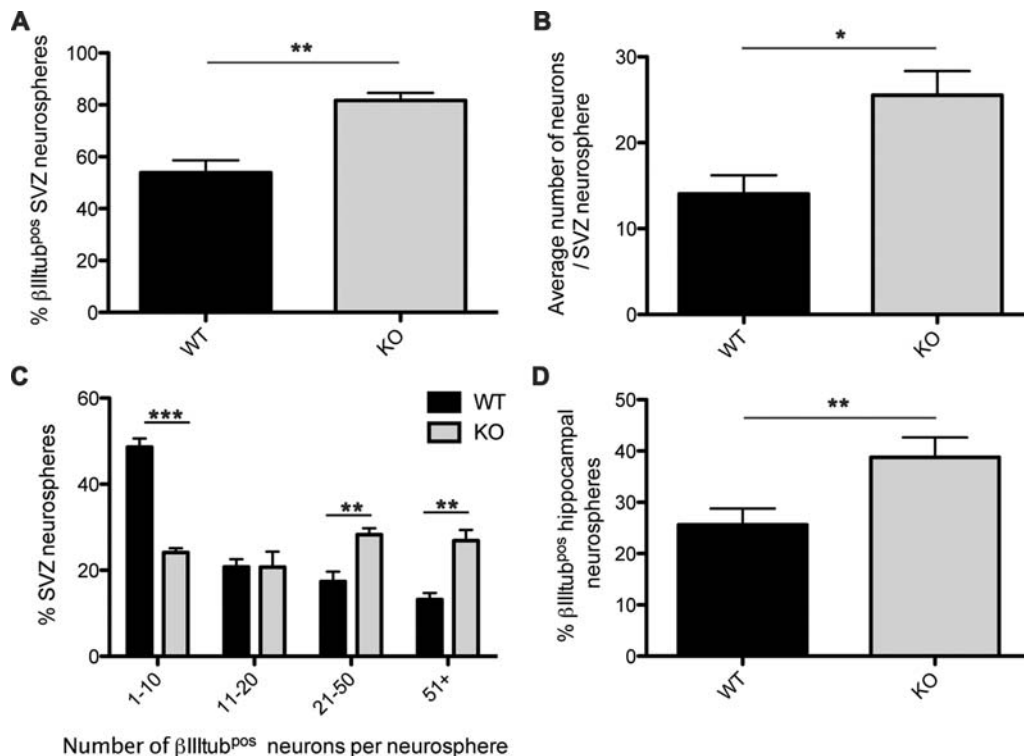


Fig. 8. SIRT1 ablation enhances the neurogenic potential of adult neural precursors. SVZ neural precursors obtained from SIRT1 deficient (KO) mice have a higher neurogenic potential than those derived from control (WT) mice. **A:** Proportion of primary SVZ neurospheres containing  $\beta$ III-tubulin expressing neurons. **B:** Average number of neurons generated per neurosphere. **C:** Neurosphere distribution based on number of the neurons within each neurosphere. **D:** Proportion of

hippocampal neurospheres containing  $\beta$ III-tubulin-expressing neurons. The neurogenic potential was enhanced in neural precursors derived from Sirt1KO animals compared with WT mice. Data are mean  $\pm$  SEM of eight WT and five Sirt1KO animals. \* $P < 0.05$ , \*\* $P < 0.01$ , \*\*\* $P < 0.001$ .

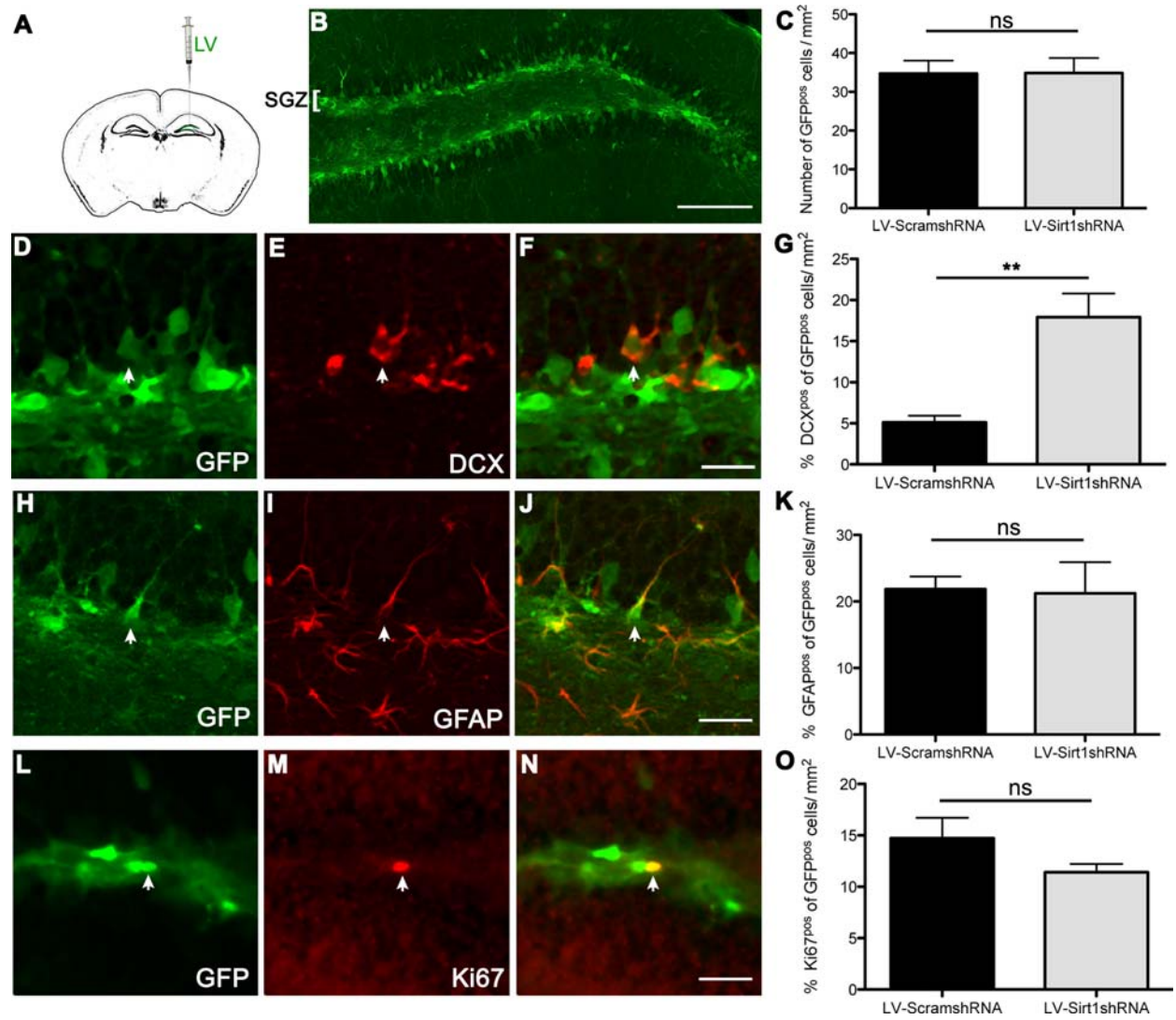
*Sirt1*<sup>KO/KO</sup> mice expressed a SIRT1 mutant protein because of the in-frame deletion of exon 4. In the protein lysate from *Sirt1*<sup>KO/KO</sup> mice, the mutant isoform of the SIRT1 protein was detected, but no wild-type protein band could be seen at 110 kDa. In heterozygous *Sirt1*<sup>KO/+</sup> neurosphere lysates, two bands corresponding to the wild-type and mutant SIRT1 isoforms were detected. The homozygous *Sirt1* knockout mice (*Sirt1*<sup>KO/KO</sup>, hereafter referred to as “Sirt1KO”) mice had a lower body mass than littermate control mice (hereafter referred to as “WT” for simplicity; WT = 25.64  $\pm$  0.94 g vs. Sirt1KO = 18.26  $\pm$  1.11 g; Student’s *t*-test,  $P < 0.001$ ;  $n = 12$  WT, 8 Sirt1KO mice). In line with this decreased body weight, the brains of the Sirt1KO mice were also lower in weight than the WT brains (WT = 41.58  $\pm$  1.51 mg vs. Sirt1KO = 31.87  $\pm$  1.46 mg; Student’s *t*-test,  $P < 0.01$ ;  $n = 5$  WT, 3 Sirt1KO brains).

To analyze the neurogenic potential of Sirt1KO neural precursors in vivo, we performed a BrdU pulse chase assay to follow the fate of newly dividing cells. Sirt1KO and control WT mice were given four pulses of BrdU, and the number of BrdU-positive cells expressing DCX was quantified 1 week after the last BrdU

pulse (Fig. 7A,B). When the number of colabeled cells along the SGZ was quantified, the results revealed a significant increase in the proportion of BrdU-positive cells that colabeled with DCX in Sirt1KO mice compared with their littermate WT controls (Student’s *t*-test,  $P < 0.01$ ; Fig. 7C), suggesting that SIRT1 loss-of-function led to a larger proportion of proliferating precursors differentiating into neurons. We also quantified cell proliferation in the SGZ by immunostaining for BrdU in the mutant mice. This analysis revealed that BrdU-positive cell numbers were comparable in Sirt1KO mice and WT littermates (Student’s *t*-test,  $P > 0.05$ ; Fig. 7D), affirming that SIRT1 signaling does not affect precursor proliferation. Having confirmed that SIRT1 loss-of-function enhanced the neurogenic capacity of proliferating neural precursors in vivo, we asked whether Sirt1KO mice had an increased number of newly formed neurons. This analysis revealed a significant increase in the total number of DCX-expressing cells in the SGZ of Sirt1KO mice compared with their WT counterparts (Student’s *t*-test,  $P < 0.05$ ; Fig. 7E).

Next, to assess the effect of SIRT1 knockout on the number of active neural precursors in the SVZ and hippocampus of Sirt1KO, we used the in vitro neuro-

F7



COLOR

Fig. 9. SIRT1 knock down increases neurogenic potential of precursors in vivo. **A**: Schematic of a coronal brain section showing the injection track terminating in the hilar region of the hippocampus. **B**: Robust GFP (green) expression can be seen in the SGZ cells infected with the lentiviral construct. **C**: Quantification of GFP-expressing cells in the SGZ of LV-ScramshRNA- and LV-Sirt1shRNA-infected mice. Both lentiviral constructs show comparable infection efficiency. Representative images showing colocalization of GFP (green) with DCX (**D-F**), GFAP (**H-J**), and Ki67 (**L-N**) cells (in red) in the SGZ (arrowheads indicate colabeled cells).

**G,K,O**: Quantification of the proportion of DCX and GFP (**G**), GFAP and GFP (**K**), and Ki67 and GFP (**O**) double-positive cells in relation to GFP-expressing cells in the SGZ. SIRT1 knock down in vivo increased the proportion of DCX-expressing newborn immature neurons relative to all GFP-expressing cells in the SGZ. Data are mean  $\pm$  SEM of eight mice per condition. ns,  $P > 0.05$ ,  $**P < 0.01$ . LV, lentiviral particles; SGZ, subgranular zone. Scale bars = 100  $\mu$ m in B; 20  $\mu$ m in F (applies to D-F); 20  $\mu$ m in J (applies to H-J); 20  $\mu$ m in N (applies to L-N).

sphere assay and quantified the total number of neurospheres generated from these precursors. For SVZ-derived neural precursors, we observed a significant decrease in the total number of primary neurospheres generated from the Sirt1KO animals ( $180.4 \pm 32.9$ ) compared with WT animals ( $326.4 \pm 23.43$ ; Student's *t*-test,  $P < 0.001$ ;  $n = 8$  WT, 5 Sirt1KO mice). However, because the brain weight of the Sirt1KO animals was lower, there was a possibility that their neurogenic

regions were also smaller and thus contained fewer cells. To investigate this, we quantified the number of neurospheres generated per  $10^5$  cells isolated from SVZ and found that the neurosphere-forming frequency in Sirt1KO mice (1 in  $1,333.89 \pm 281.19$  cells) and their WT littermates (1 in  $840.43 \pm 98.55$  cells) did not differ significantly (Student's *t*-test,  $P > 0.05$ ). Similarly to the SVZ, the total number of neurospheres derived from the hippocampus of Sirt1KO mice ( $36.5 \pm 2.94$ ) was also

dramatically reduced compared with that obtained from control WT animals ( $15.25 \pm 2.14$ ; Student's *t*-test,  $P < 0.01$ ;  $n = 9$  WT, 6 Sirt1KO mice). However, there was no significant difference in the neurosphere-forming frequency of hippocampal cells from Sirt1KO (1 in  $15,108.19 \pm 3,754.06$  cells) vs. WT mice (1 in  $9,985.42 \pm 524.07$  cells; Student's *t*-test,  $P > 0.05$ ).

F8 Finally, to ascertain that the enhanced neurogenesis observed in Sirt1KO mice in vivo was a direct consequence of increased neurogenic potential of Sirt1KO neural precursors, we tested the neuron-generating capacity of SVZ and hippocampal neural precursors by performing the in vitro differentiation assay with Sirt1KO and WT neurospheres. A significantly higher proportion of Sirt1KO SVZ neurospheres generated  $\beta$ III-tubulin-expressing neurons (Student's *t*-test,  $P < 0.001$ ; Fig. 8A). In addition, the average number of neurons generated by each Sirt1KO neurosphere was also significantly higher than that produced by the WT neurospheres (Student's *t*-test,  $P < 0.05$ ; Fig. 8B). Furthermore, the distribution profile of the Sirt1KO neurospheres revealed a significant bias toward a higher number of differentiated neurons per neurosphere compared with the distribution profile of the WT neurospheres (two-way ANOVA,  $P < 0.001$ ; Fig. 8C). We also investigated whether hippocampal neural precursors from Sirt1KO mice exhibited an enhanced intrinsic neurogenic potential. In line with our previous data, we observed a significant increase in the number of Sirt1KO hippocampal neurospheres that gave rise to neuronal progeny (Student's *t*-test,  $P < 0.05$ ; Fig. 8D).

### Lentivirus-Mediated SIRT1 Knock Down Leads to Increased Numbers of Newborn Neurons In Vivo

F9 Although the Sirt1KO mice were invaluable for studying the in vivo role of SIRT1 in adult hippocampal precursors, the observed phenotype in these mice could be due to either compensatory mechanisms arising during development or secondary effects consequent to germline deletion of Sirt1. To address specifically the effects of in vivo SIRT1 knock down in the adult SGZ, we used the lentiviral system to knock down SIRT1 expression in neural precursors residing within the SGZ by administering LV-Sirt1shRNA stereotaxically into the hilar region (Fig. 9A). Control mice were injected with LV-ScramshRNA. The animals were sacrificed after a 2-week period to permit transgene expression and to allow the infected cells a window of opportunity in which to differentiate. To assess the spread of lentiviral particles within the brain, we analyzed brain sections of mice infected with lentiviral vectors for distribution of GFP-expressing cells. Two weeks after injection of the vectors, GFP-expressing cells were mostly confined to the SGZ, with some GFP-positive cells seen in the granule cell layer of the dentate gyrus (Fig. 9B). No GFP-positive cells were detected in any other area of the hippocampus or in any other brain area. Evaluation of the infection efficiency of LV-Sirt1shRNA and LV-

ScramshRNA, by quantification of the total number of GFP-expressing cells per square millimeter of the SGZ, revealed no significant difference in the number of GFP-expressing cells (Student's *t*-test,  $P > 0.05$ ; Fig. 9C), suggesting that both constructs had similar infection efficiencies. Such selective manipulation of SIRT1 activity in vivo combined with the fluorescence tagging of the successfully silenced cells allowed us to test our in vitro findings in vivo. To evaluate potential changes in neuronal differentiation, we quantified the number of GFP-expressing cells in the SGZ that colabeled with the early neuronal marker DCX. This revealed a marked fourfold increase in colabeled GFP-expressing and DCX-positive cells in the SGZ of LV-Sirt1shRNA-infected mice compared with control LV-ScramshRNA-infected mice (Student's *t*-test,  $P < 0.01$ ; Fig. 9D–G). We next questioned whether SIRT1 knock down was specifically enhancing the neurogenic potential of neural precursors or whether it was also influencing their differentiation into the other predominant neural precursor progeny, glia. To assess this, we analyzed the proportion of GFP-expressing cells that colabeled with the astroglial marker GFAP and found no difference between the LV-Sirt1shRNA- and control LV-ScramshRNA-injected mice (Student's *t*-test,  $P > 0.05$ ; Fig. 9H–K).

To rule out any secondary effects caused by increased precursor proliferation, we quantified the percentage of GFP-expressing cells that coexpressed Ki67, a marker for proliferation. No difference was found between mice injected with scrambled control and mice injected with LV-Sirt1shRNA (Student's *t*-test,  $P > 0.05$ ; Fig. 9L–O), suggesting that SIRT1 knock down did not affect proliferation. Moreover, to ascertain that the observed increase in DCX-expressing cells was a result of enhanced differentiation and not survival, we performed a 2-week-long BrdU pulse chase experiment with LV-Sirt1shRNA- and LV-ScramshRNA-injected mice. This analysis revealed no difference in either the total number of BrdU-positive cells per square millimeter of SGZ (LV-Sirt1shRNA =  $16.81 \pm 0.77$ , LV-ScramshRNA =  $16.49 \pm 1.10$ ; Student's *t*-test,  $P > 0.05$ ;  $n = 8$  sections per brain, four brains per condition) or the proportion of GFP-expressing cells that coexpressed BrdU in the SGZ (LV-Sirt1shRNA =  $1.55 \pm 0.22$ , LV-ScramshRNA =  $1.73 \pm 0.31$ ; Student's *t*-test,  $P > 0.05$ ;  $n = 8$  sections per brain, four brains per condition), suggesting that SIRT1 knock down had no effect on the survival of newborn cells.

## DISCUSSION

Here we provide the first evidence of a role for SIRT1 in regulating adult neurogenesis. Our results reveal that SIRT1 is strongly expressed by proliferating neural precursors in both neurogenic regions of the adult mouse brain, as demonstrated by colabeling with the proliferation marker Ki67. Furthermore, we demonstrate that SIRT1 has no effect on precursor proliferation but inhibits their differentiation into a neuronal cell type, as

evidenced by the finding that RNAi-mediated knock down of SIRT1 enhanced neuronal differentiation of both SVZ- and hippocampus-derived adult neural precursors *in vitro*. Similarly, neural precursors derived from the SVZ and hippocampus of genetically ablated Sirt1KO mice also showed no change in proliferation but exhibited intrinsically enhanced neurogenic potential, as demonstrated by an increased number of  $\beta$ III tubulin-positive neuronal progeny in differentiated Sirt1KO neurospheres *in vitro*. It may be that loss-of-function of Sirt1 may result in a greater number of cycling precursors differentiating into neurons at the expense of other cell types, or alternatively it may influence the differentiation rate of precursor cells by accelerating their exit from cell cycle toward neuronal fate.

Consistent with our *in vitro* findings, loss of SIRT1 function *in vivo*, either through lentiviral-mediated knock down or through genetic elimination, resulted in enhanced neurogenic potential of hippocampal precursors. In Sirt1KO animals, a higher percentage of proliferating precursors was committed to a neuronal fate, as shown by BrdU and DCX coexpression and the finding that there was a significant increase in the total number of newborn DCX-expressing cells within the SGZ, demonstrating increased hippocampal neurogenesis. The DCX-positive lineage contains proliferating cells as well as more mature neurons. Whether Sirt1 specifically regulates the DCX-positive proliferating neuroblast population or newborn neuron pool is presently not clear; however, the increase in DCX-positive neurons observed following lentivirus-mediated SIRT1 downregulation in the adult SGZ provides further evidence that SIRT1 has a direct inhibitory effect on adult neural precursor differentiation. Future studies utilizing a panel of cell-type-specific marker expression will provide insights into the stage-specific effects of Sirt1 in regulating quiescent vs. active precursor pools during adult neurogenesis.

In contrast to our findings, a study by Hisahara and colleagues (2008) suggested that increased Sirt1 signaling enhanced neuronal differentiation of the embryonic precursor cells by binding to nuclear receptor corepressor (NCoR) and repressing the expression of Hes1. There are several factors that may underlie these contrasting observations, including age of animals, location from which precursor cells were isolated, differentiation conditions, and temporal window of examination. Importantly, the study by Hisahara and colleagues failed to examine whether the effects of Sirt1 inhibitors in reducing neuronal differentiation were mediated via a Sirt1-dependent mechanism. Overall, it is possible that Sirt1 has different regulatory functions in different cell types and biological contexts and that Sirt1 function is dependent on the extrinsic factors presented by the cellular microenvironment.

The inhibitory action of SIRT1 was further confirmed by overexpression of SIRT1, which had no effect on proliferation but strongly inhibited neuronal differentiation of SVZ as well as hippocampal neural precursors. In line with the decrease in neuronal differentiation

observed with SIRT1 overexpression, increasing the enzymatic activity of SIRT1 with Resveratrol treatment also led to decreased neuronal differentiation of both SVZ and hippocampal neural precursors. Resveratrol has previously been shown to mediate its biological effects through both SIRT1-dependent and SIRT1-independent mechanisms (Baur, 2009; Pallas et al., 2009; Ogawa et al., 2011; Kelly, 2011). Here we show that the inhibitory effect of Resveratrol on neuronal differentiation is mediated primarily by a SIRT1-dependent mechanism, insofar as SIRT1 knock down restored the neurogenic potential of Resveratrol-treated precursors.

Taken together, the findings described above demonstrate that SIRT1 signaling affects the neurogenic potential of both hippocampal and SVZ precursors. This commonality of mechanism is striking given that adult SVZ and SGZ neural precursors display distinct cellular and functional properties, with SVZ neural precursors exhibiting substantial proliferative activity and high neurogenic potential *in vitro* (Reynolds and Weiss, 1996), whereas SGZ precursors exhibit limited proliferative capacity and reduced neurogenic capacity (Bull and Bartlett, 2005). Moreover, in contrast to the SVZ, the SGZ contains a large population of latent precursors that can be activated by signals that mimic synaptic activity *in vitro* (Walker et al., 2008). However, despite the inherent differences in the precursor populations residing in these two niches, our results suggest that SIRT1 signaling represents a conserved mechanism used by adult neural precursors to regulate neuronal differentiation negatively. Previous studies have implicated the role of other class I and II HDACs in inhibiting neuronal differentiation of adult neural precursors (Hsieh et al., 2004; Siebzehnruhl et al., 2007; Kim et al., 2009), whereas histone acetyl transferases such as Querkopf have been shown to promote neuronal differentiation (Merson et al., 2006). Given that, in Sirt1 knock down animals, enough homeostatic and compensatory mechanisms are still in place to allow for the development of a grossly normal hippocampus, it is possible that several HDACs along with other members of the Sirt1 family, Sirt2–Sirt7, act together to regulate neuronal differentiation of proliferating neural precursors and can therefore partially compensate for Sirt1 loss-of-function.

Given the numerous studies that show a correlation between hippocampal-dependent learning and adult hippocampal neurogenesis (Gould et al., 1999; van Praag et al., 1999; Lemaire et al., 2000; Matsumori et al., 2006; Anderson et al., 2010), it is intriguing that two recent studies, using the same nestin-Cre-mediated SIRT1 knock down experimental strategy, indicated that SIRT1 ablation in the brain results in deficits in hippocampal-dependent learning and memory (Gao et al., 2010; Michan et al., 2010). Gao and colleagues (2010) ascribed the behavioral defects to a corresponding decrease in synaptic density and a reduction in long-term potentiation. Our analysis of SIRT1 expression shows that SIRT1 is robustly expressed in mature neurons within the granule cell layer of the dentate gyrus,

raising the possibility of an additional function for SIRT1 in mature neurons in modulating synaptic plasticity. Future studies utilizing a conditional genetic approach will aid in determining the effects of selective SIRT1 knock down in adult precursors on hippocampal-dependent learning and memory tasks.

Our results suggest that SIRT1 levels within proliferating precursors represent a crucial checkpoint that regulates neuronal differentiation potential. In agreement with this, we find that, although SIRT1 is strongly expressed by proliferating neural precursors, its expression is significantly downregulated during the differentiation of neurospheres in vitro. It has been shown that SIRT1 levels decrease at the onset of neuronal differentiation during embryonic development (Sakamoto et al., 2004). Downregulation of SIRT1 protein with cell cycle withdrawal has also previously been reported for mouse embryonic fibroblasts (Sasaki et al., 2006). Furthermore, our qRT-PCR analysis revealed a tenfold decrease in Sirt1 mRNA levels in differentiated neurospheres, strongly suggesting that downregulation of SIRT1 is primarily regulated at the level of transcription.

An important question that arises from our findings is, What regulates SIRT1? One of the strongest regulators of SIRT1 activity is the coenzyme NAD<sup>+</sup>. Given that the deacetylase reaction catalyzed by SIRT1 is NAD<sup>+</sup> dependent, SIRT1 activity is intimately linked to the [NAD<sup>+</sup>]/[NADH] ratio within a cell, which represents its redox state (Landry et al., 2000). It has been shown that differentiation of skeletal muscle cells is accompanied by modifications of the [NAD<sup>+</sup>]/[NADH] ratio, which exerts regulatory effects on SIRT1 (Fulco et al., 2008). Recently, adult neural stem cells from the SVZ have been shown to have a high redox potential owing to high levels of reactive oxidative species (Le Belle et al., 2010). It is conceivable that, in adult neural precursors, SIRT1 responds to the redox state of a cell, through its dependence on NAD<sup>+</sup>, to regulate processes related to cell cycle and differentiation. In support of this, Prozorovski and colleagues (2008) have shown that redox state regulates neuronal differentiation in embryonic neural precursors through a SIRT1-dependent mechanism. SIRT1 was shown to bind to Hes1 under mild oxidative conditions in embryonic neural precursors, resulting in transcriptional inhibition of Mash1, and consequent inhibition of neuronal differentiation. SIRT1 has also previously been shown to interact with Hes1 and repress downstream target promoters (Takata and Ishikawa, 2003). Hes1 is well known to inhibit neuronal differentiation of embryonic stem cells during development (Ohtsuka et al., 1999; Nakamura et al., 2000; Kobayashi et al., 2009; Zhang et al., 2009), and its expression has been demonstrated in SVZ- and SGZ-derived adult neural precursors (Stump et al., 2002; Sui et al., 2009; Wang et al., 2009). Given the expression pattern of Hes1, its known role in regulating neuronal differentiation, and the evidence for interaction between Hes1 and SIRT1, it appears likely that SIRT1 associates with Hes1 in adult neural precursors to form a corepres-

or complex that inhibits neurogenic genes and prevents neuronal differentiation. Together the data from this study provide compelling evidence for the role of SIRT1 in regulating adult neural precursor activity and reveal SIRT1 as a negative regulator of the neurogenic potential of these cells.

## ACKNOWLEDGMENTS

We thank Prof. Linda Richards for providing the nestin-Cre transgenic mice and Dr. Nigel McMillan for providing the lentiviral constructs. We also thank Rowan Tweedale and Ashley Cooper for editorial assistance. The funders had no role in study design, data collection and analysis, decision to publish, or preparation of the manuscript. S.S. was supported by an Endeavour Asia Award and International Postgraduate Research Scholarship.

## REFERENCES

- Agathocleous M, Iordanova I, Willardson MI, Xue XY, Vetter ML, et al. 2009. A directional Wnt/beta-catenin-Sox2-proneural pathway regulates the transition from proliferation to differentiation in the *Xenopus* retina. *Development* 136:3289–3299.
- Anderson ML, Sisti HM, Curlik DM 2nd, Shors TJ. 2010. Associative learning increases adult neurogenesis during a critical period. *Eur J Neurosci* 33:175–181.
- Balasubramanian V, Boddeke E, Bakels R, Kust B, Kooistra S, et al. 2006. Effects of histone deacetylation inhibition on neuronal differentiation of embryonic mouse neural stem cells. *Neuroscience* 143:939–951.
- Ballas N, Mandel G. 2005. The many faces of REST oversee epigenetic programming of neuronal genes. *Curr Opin Neurobiol* 15:500–506.
- Baur JA. 2009. Biochemical effects of SIRT1 activators. *Biochim Biophys Acta* 1804:1626–1634.
- Borra MT, Smith BC, Denu JM. 2005. Mechanism of human SIRT1 activation by Resveratrol. *J Biol Chem* 280:17187–17195.
- Briscoe J. 2009. Making a grade: Sonic Hedgehog signalling and the control of neural cell fate. *EMBO J* 28:457–465.
- Bull ND, Bartlett PF. 2005. The adult mouse hippocampal progenitor is neurogenic but not a stem cell. *J Neurosci* 25:10815–10821.
- Calvanese V, Lara E, Suarez-Alvarez B, Abu Dawud R, Vazquez-Chantada M, et al. 2010. Sirtuin 1 regulation of developmental genes during differentiation of stem cells. *Proc Natl Acad Sci U S A* 107:13736–13741.
- Cohen HY, Miller C, Bitterman KJ, Wall NR, Hekking B, et al. 2004. Calorie restriction promotes mammalian cell survival by inducing the SIRT1 deacetylase. *Science* 305:390–392.
- Dull T, Zufferey R, Kelly M, Mandel RJ, Nguyen M, et al. 1998. A third-generation lentivirus vector with a conditional packaging system. *J Virol* 72:8463–8471.
- Follenzi A, Sabatino G, Lombardo A, Boccaccio C, Naldini L. 2002. Efficient gene delivery and targeted expression to hepatocytes in vivo by improved lentiviral vectors. *Hum Gene Ther* 13:243–260.
- Fremont L. 2000. Biological effects of Resveratrol. *Life Sci* 66:663–673.
- Fulco M, Cen Y, Zhao P, Hoffman EP, McBurney MW, et al. 2008. Glucose restriction inhibits skeletal myoblast differentiation by activating SIRT1 through AMPK-mediated regulation of Nampt. *Dev Cell* 14:661–673.
- Gao J, Wang W-Y, Mao Y-W, Gräff J, Guan J-S, et al. 2010. A novel pathway regulates memory and plasticity via SIRT1 and miR-134. *Nature* 466:1105–1109.




- Gould E, Beylin A, Tanapat P, Reeves A, Shors TJ. 1999. Learning enhances adult neurogenesis in the hippocampal formation. *Nat Neurosci* 2:260–265.
- Haigis MC, Guarente LP. 2006. Mammalian sirtuins—emerging roles in physiology, aging, and calorie restriction. *Genes Dev* 20:2913–2921.
- Han MK, Song EK, Guo Y, Ou X, Mantel C, et al. 2008. SIRT1 regulates apoptosis and Nanog expression in mouse embryonic stem cells by controlling p53 subcellular localization. *Cell Stem Cell* 2:241–251.
- Hirabayashi Y, Gotoh Y. 2010. Epigenetic control of neural precursor cell fate during development. *Nat Rev Neurosci* 11:377–388.
- Hisahara S, Chiba S, Matsumoto H, Tanno M, Yagi H, et al. 2008. Histone deacetylase SIRT1 modulates neuronal differentiation by its nuclear translocation. *Proc Natl Acad Sci U S A* 105:15599–15604.
- Howitz KT, Bitterman KJ, Cohen HY, Lamming DW, Lavu S, et al. 2003. Small molecule activators of sirtuins extend *Saccharomyces cerevisiae* lifespan. *Nature* 425:191–196.
- Hsieh J, Eisch AJ. 2010. Epigenetics, hippocampal neurogenesis, and neuropsychiatric disorders: unraveling the genome to understand the mind. *Neurobiol Dis* 39:73–84.
- Hsieh J, Gage FH. 2004. Epigenetic control of neural stem cell fate. *Curr Opin Genet Dev* 14:461–469.
- Hsieh J, Nakashima K, Kuwabara T, Mejia E, Gage FH. 2004. Histone deacetylase inhibition-mediated neuronal differentiation of multipotent adult neural progenitor cells. *Proc Natl Acad Sci U S A* 101:16659–16664.
- Jennemann R, Sandhoff R, Wang S, Kiss E, Gretz N, et al. 2005. Cell-specific deletion of glucosylceramide synthase in brain leads to severe neural defects after birth. *Proc Natl Acad Sci U S A* 102:12459–12464.
- Juliandi B, Abematsu M, Nakashima K. 2010. Chromatin remodeling in neural stem cell differentiation. *Curr Opin Neurobiol* 20:408–415.
- Kelly GS. 2011. A review of the sirtuin system, its clinical implications, and the potential role of dietary activators like Resveratrol: part 2. *Altern Med Rev* 15:313–328.
- Kim HJ, Leeds P, Chuang DM. 2009. The HDAC inhibitor, sodium butyrate, stimulates neurogenesis in the ischemic brain. *J Neurochem* 110:1226–1240.
- Kobayashi T, Mizuno H, Imayoshi I, Furusawa C, Shirahige K, et al. 2009. The cyclic gene *Hes1* contributes to diverse differentiation responses of embryonic stem cells. *Genes Dev* 23:1870–1875.
- Kohyama J, Kojima T, Takatsuka E, Yamashita T, Namiki J, et al. 2008. Epigenetic regulation of neural cell differentiation plasticity in the adult mammalian brain. *Proc Natl Acad Sci U S A* 105:18012–18017.
- Kulkarni VA, Jha S, Vaidya VA. 2002. Depletion of norepinephrine decreases the proliferation, but does not influence the survival and differentiation, of granule cell progenitors in the adult rat hippocampus. *Eur J Neurosci* 16:2008–2012.
- Landry J, Slama JT, Sternglanz R. 2000. Role of NAD<sup>+</sup> in the deacetylase activity of the SIR2-like proteins. *Biochem Biophys Res Commun* 278:685–690.
- Le Belle JE, Orozco NM, Paucar AA, Saxe JP, Mottahedeh J, et al. 2010. Proliferative neural stem cells have high endogenous ROS levels that regulate self-renewal and neurogenesis in a PI3K/Akt-dependant manner. *Cell Stem Cell* 8:59–71.
- Lemaire V, Koehl M, Le Moal M, Abrous DN. 2000. Prenatal stress produces learning deficits associated with an inhibition of neurogenesis in the hippocampus. *Proc Natl Acad Sci U S A* 97:11032–11037.
- Li H, Rajendran GK, Liu N, Ware C, Rubin BP, et al. 2007. SirT1 modulates the estrogen-insulin-like growth factor-1 signaling for post-natal development of mammary gland in mice. *Breast Cancer Res* 9:R1.
- Lyssiotis CA, Walker J, Wu C, Kondo T, Schultz PG, et al. 2007. Inhibition of histone deacetylase activity induces developmental plasticity in oligodendrocyte precursor cells. *Proc Natl Acad Sci U S A* 104:14982–14987.
- Matsumori Y, Hong SM, Fan Y, Kayama T, Hsu CY, et al. 2006. Enriched environment and spatial learning enhance hippocampal neurogenesis and salvages ischemic penumbra after focal cerebral ischemia. *Neurobiol Dis* 22:187–198.
- Merson TD, Dixon MP, Collin C, Rietze RL, Bartlett PF, et al. 2006. The transcriptional coactivator Querkopf controls adult neurogenesis. *J Neurosci* 26:11359–11370.
- Michan S, Li Y, Chou MM-H, Parrella E, Ge H, et al. 2010. SIRT1 is essential for normal cognitive function and synaptic plasticity. *J Neurosci* 30:9695–9707.
- Nakamura Y, Sakakibara S, Miyata T, Ogawa M, Shimazaki T, et al. 2000. The bHLH gene *hes1* as a repressor of the neuronal commitment of CNS stem cells. *J Neurosci* 20:283–293.
- Ogawa T, Wakai C, Saito T, Murayama A, Mimura Y, et al. 2011. Distribution of the longevity gene product, SIRT1, in developing mouse organs. *Congenit Anom* 51:70–79.
- Ohtsuka T, Ishibashi M, Gradwohl G, Nakanishi S, Guillemot F, et al. 1999. *Hes1* and *Hes5* as notch effectors in mammalian neuronal differentiation. *EMBO J* 18:2196–2207.
- Pallas M, Casadesus G, Smith MA, Coto-Montes A, Pelegri C, et al. 2009. Resveratrol and neurodegenerative diseases: activation of SIRT1 as the potential pathway toward neuroprotection. *Curr Neurovasc Res* 6:70–81.
- Pervaiz S, Holme AL. 2009. Resveratrol: its biologic targets and functional activity. *Antiox Redox Signal* 11:2851–2897.
- Prozorovski T, Schulze-Topphoff U, Glumm R, Baumgart J, Schroter F, et al. 2008. *Sirt1* contributes critically to the redox-dependent fate of neural progenitors. *Nat Cell Biol* 10:385–394.
- Reynolds BA, Weiss S. 1992. Generation of neurons and astrocytes from isolated cells of the adult mammalian central nervous system. *Science* 255:1707–1710.
- Reynolds BA, Weiss S. 1996. Clonal and population analyses demonstrate that an EGF-responsive mammalian embryonic CNS precursor is a stem cell. *Dev Biol* 175:1–13.
- Sakamoto J, Miura T, Shimamoto K, Horio Y. 2004. Predominant expression of Sir2alpha, an NAD-dependent histone deacetylase, in the embryonic mouse heart and brain. *FEBS Lett* 556:281–286.
- Sasaki T, Maier B, Bartke A, Scoble H. 2006. Progressive loss of SIRT1 with cell cycle withdrawal. *Aging Cell* 5:413–422.
- Schneider JW, Gao Z, Li S, Farooqi M, Tang TS, et al. 2008. Small-molecule activation of neuronal cell fate. *Nat Chem Biol* 4:408–410.
- Siebzehnrubl FA, Buslei R, Eyupoglu IY, Seufert S, Hahnen E, et al. 2007. Histone deacetylase inhibitors increase neuronal differentiation in adult forebrain precursor cells. *Exp Brain Res* 176:672–678.
- Stump G, Durrer A, Klein AL, Lutolf S, Suter U, et al. 2002. Notch1 and its ligands Delta-like and Jagged are expressed and active in distinct cell populations in the postnatal mouse brain. *Mech Dev* 114:153–159.
- Sui Y, Zhang Z, Guo Y, Sun Y, Zhang X, et al. 2009. The function of Notch1 signaling was increased in parallel with neurogenesis in rat hippocampus after chronic fluoxetine administration. *Biol Pharm Bull* 32:1776–1782.
- Takata T, Ishikawa F. 2003. Human Sir2-related protein SIRT1 associates with the bHLH repressors HES1 and HEY2 and is involved in HES1- and HEY2-mediated transcriptional repression. *Biochem Biophys Res Commun* 301:250–257.
- Tiscornia G, Singer O, Verma IM. 2006. Design and cloning of lentiviral vectors expressing small interfering RNAs. *Nat Protoc* 1:234–240.
- Tronche F, Kellendonk C, Kretz O, Gass P, Anlag K, et al. 1999. Disruption of the glucocorticoid receptor gene in the nervous system results in reduced anxiety. *Nat Genet* 23:99–103.

18 Saharan et al.

- van Praag H, Christie BR, Sejnowski TJ, Gage FH. 1999. Running enhances neurogenesis, learning, and long-term potentiation in mice. *Proc Natl Acad Sci U S A* 96:13427–13431.
- Walker TL, White A, Black DM, Wallace RH, Sah P, et al. 2008. Latent stem and progenitor cells in the hippocampus are activated by neural excitation. *J Neurosci* 28:5240–5247.
- Wallenborg K, Vlachos P, Eriksson S, Huijbregts L, Arnér ESJ, et al. 2009. Red wine triggers cell death and thioredoxin reductase inhibition: effects beyond Resveratrol and SIRT1. *Exp Cell Res* 315:1360–1371.
- Wang X, Mao X, Xie L, Greenberg DA, Jin K. 2009. Involvement of Notch1 signaling in neurogenesis in the subventricular zone of normal and ischemic rat brain in vivo. *J Cereb Blood Flow Metab* 29:1644–1654.
- Wen S, Li H, Liu J. 2009. Epigenetic background of neuronal fate determination. *Prog Neurobiol* 87:98–117.
- Wexler EM, Paucer A, Kornblum HI, Palmer TD, Geschwind DH. 2009. Endogenous Wnt signaling maintains neural progenitor cell potency. *Stem Cells* 27:1130–1141.
- Yu IT, Park JY, Kim SH, Lee JS, Kim YS, et al. 2009. Valproic acid promotes neuronal differentiation by induction of proneural factors in association with H4 acetylation. *Neuropharmacology* 56:473–480.
- Zhang C, Zhang Z, Shu H, Liu S, Song Y, et al. 2009. The modulatory effects of bHLH transcription factors with the Wnt/beta-catenin pathway on differentiation of neural progenitor cells derived from neonatal mouse anterior subventricular zone. *Brain Res* 1315:1–10.



Author Proof

AQ1: Pls define the scale bar in E. 



**Author Proof**